LICENCE TO McMASTER UNIVERSITY

This Thesis has been written
[Thesis, Project Report, etc.]

by Anastasia Fair for
[Full Name(s)]

Undergraduate course number 4K06 at McMaster University under the supervision/direction of Dr. W. Morris and Dr. Clifford.

In the interest of furthering teaching and research, I/we hereby grant to McMaster University:

1. The ownership of 6 copy(ies) of this work;
2. A non-exclusive licence to make copies of this work, (or any part thereof) the copyright of which is vested in me/us, for the full term of the copyright, or for so long as may be legally permitted. Such copies shall only be made in response to a written request from the Library or any University or similar institution.

I/we further acknowledge that this work (or a surrogate copy thereof) may be consulted without restriction by any interested person.

W A Morris
Signature of Witness, Supervisor

Anastasia Fair
Signature of Student

May 17/96
date

(This Licence to be bound with the work)

PETROLOGICAL AND MAGNETIC FABRIC IN THE SOUTH REGION OF THE KILLARNEY IGNEOUS COMPLEX

PETROLOGICAL AND MAGNETIC FABRIC IN THE SOUTH REGION OF THE KILLARNEY IGNEOUS COMPLEX

BY

ANASTASIA FAIR

A Thesis

Submitted to the Department of Geology

in Partial Fulfilment of the Requirements for the

Degree Bachelor of Science

McMaster University

April, 1996

BACHELOR OF SCIENCE, (1996) McMaster University,
(Geology Major) Hamilton, Ontario

TITLE: Petrological and Magnetic Fabric in the South Region of the Killarney Igneous Complex

AUTHOR: Anastasia Fair

SUPERVISORS: Dr. W. A. Morris and Dr. P. M. Clifford

Abstract

Forty-Three cores were collected from the region of the Killarney Igneous Complex, southeast of the town Killarney. These cores were analysed by measuring geophysical properties such as bulk susceptibility, percent anisotropy, magnetic foliation and lineation and remanence. The magnetic fabric measured indicated a regional fabric. In some areas the fabric was completely overprinted due to localised deformation. Measured remanence may make it possible to determine the effect of previous deformations; however, none was seen in this study.

The petrological fabric was also investigated by taking thin sections perpendicular to the long axis of the core. Again it was possible to see a regional and localized deformation pattern due to reduced grain size, grain alignment and recrystallization.

Measurements collected from the samples determined that both the magnetic fabric and petrological fabric showed indications of being near areas of greater deformational intensities. A relationship was then established between the magnetic fabric and petrological fabric on a fine scale. This relationship may aid in determining direction and extent of deformation in the rock bodies when it is not easily identifiable in the field.

Acknowledgements

I would like to thank Dr. P.M. Clifford for suggesting such an interesting place to study and for his interpretations of the structural processes which had occurred. My sincere gratitude goes to Dr. W. A. Morris for seeing the potential in my ability to grasp geophysics and allowing me to become a student in his lab. His constant guidance, patience and support have been a great help throughout my thesis study and the years here at McMaster University.

Len Zwicker and Jack Whorwood have to thanked also for their technical support, as I could not have completed this thesis and its presentation without their expertise.

The geophysics lab has been a tremendous help, especially Edna Mueller, who for the past two years has given me nothing but support, academical, emotionally and technically. Susanne, George and Sean, also deserve a big thanks, who have also always been there for me with their ideas, laughter and friendship.

Most of all, I thank Ken Fair, who has been standing by me for the last five years while I chased my dream. Without your support I would not be who and where I am today.

Table of Contents

List of Figures

INTRODUCTION:

Anisotropy of magnetic susceptibility (AMS) is a well established method for regional petrofabric analysis. This method is sensitive to low percentages of anisotropy, and so is a valuable method for measuring magnetic fabric on a finite scale. Spatial variations of magnetic fabric ellipsoid shapes and their intensities, as determined through AMS, have been used to determine structural events. The effects from such a process can be seen with AMS when it is not easily identified in the country rock. Examples of where AMS has been used; in the identification of emplacement flow patterns in both granitic and basic plutons, locate regions of enhanced structural deformation, and subsequent deformation which has occurred in sediments.

Cruden and Launeau (1994) studied the magnetic fabric of the Archean Lebel Stock to determine the magnetic foliation and possible source of its orientation. By plotting the magnetic fabric and investigating the petrology, they were able to distinguish a preferred orientation of the mineralogy which may have been acquired during magmatic to sub-magmatic flow. The Exeter Pluton was investigated by Birch (1979) for a similar reasons, as there was no direct evidence in the field of any signs of foliation. From the samples he collected and analysed it became clear that the majority of the magnetic fabric was from the original flow motion of the pluton body emplacement. Changes in orientation were seen in some samples, which may have been from postemplacement strain, but none of this strain was seen in the field. Further studies were conducted by Park et al (1988) and Benn (1993) which indicated how the regional magnetic fabric can be overprinted by localised enhanced deformation. Park et al (1988) collected samples from the Mealy Diabase Dykes from Labrador and through the use of AMS, defined correlations between the magnetic fabric and deformational effects in the rock. Benn (1993) applied numerical models to the overprinting of magnetic fabrics in granites by small strains. He was able to determine the minimum amount of strain required to significantly modify pre-existing AMS, (approximately 10% strain in the pure shear regime). Initial orientation of the minerals present were also recognized as an important factor in the changes of the magnetic fabric through strain. He concluded that small amounts of strain are able to combine or overprint the original AMS fabric depending on the strain type and the original fabric.

Deformation in sediments was studied by Hirt et al (1993) using the AMS technique. They examined the sediments in the Onaping Formation to determine if they had undergone deformation since their original deposition. By correlating their finite strain results and AMS measurements, they were able to establish a deformational sequence of events and proposed an original round shape of the Sudbury Basin.

Hargraves et al (1991) went a step further then these studies, and looked at the parameters which may cause rock samples to have specific magnetic properties. They believed that since silicates would crystallize first the magnetite's crystallization could only occur in the residual magma volumes remaining. From their study they were able to show that "...AMS in pristine igneous rocks is a direct or indirect reflection of preexisting silicate fabric."

Most of this past research has been concentrated on the application of magnetic fabric to regional structural studies. In this study I have set out to determine a relationship between petrology and magnetic fabric and their correlation to deformation on a much finer scale.

Background:

Anisotropy of magnetic susceptibility is the measurement of the magnetic fabric in the rock sample. It measures the bulk susceptibility, percent anisotropy and intensities and orientation of the maximum, intermediate and minimum axes creating a magnetic ellipse. These axis are the values of magnetic intensities in the maximum, intermediate and minimum direction. This total fabric measured from any unit volume of rock represents the summation of the effects from all the magnetic minerals present. Original fabric, associated with emplacement and additional structural fabrics (related to regional deformation events) combine to represent the total fabric measured. More specifically, the crystal shape, crystal fabric and crystal alignment of the magnetic minerals present in the rock sample define the magnetic fabric. The crystal shape refers to the physical geometry of the mineral, such as equant, euhedral or elongate crystals. Crystal alignment indicates the orientation of the mineral and its interaction with other individual minerals. As with equant crystals in an elongate, linear pattern producing an anisotropy. Previous studies by Davis and Evans (1979) indicated that when magnetic grains are allowed to interact with each other, a greater susceptibility and anisotropy was seen. Fabric of the crystal is determined by its internal structure composition. For example a crystalline structure may impose its own fabric as in the basal plane of hematite which is more magnetically susceptible. The state of the electrons in the outer most shell dictate whether the mineral will be paramagnetic (paired electrons) or ferromagnetic (unpaired). Ferromagnetism dominates over paramagnetism, but occurs in smaller quantities. The magnetic fabric may then be represented by the paramagnetic mineralogy when it occurs in large quantities.

Remanence, which was examined in this study, only refers to the ferromagnetic minerals present in the samples. Unlike paramagnetic minerals, they are able to retain a magnetic field once the applied field is removed. Genesis of remanence can occur in nature from chemical changes, depositional settings, thermal mechanisms and other such processes.

Study Area:

The Killarney Igneous Complex is one of five pluton bodies immediately north of the Grenville Front. It is a lenticular body trending NE/SW (figure 1). Wanless and

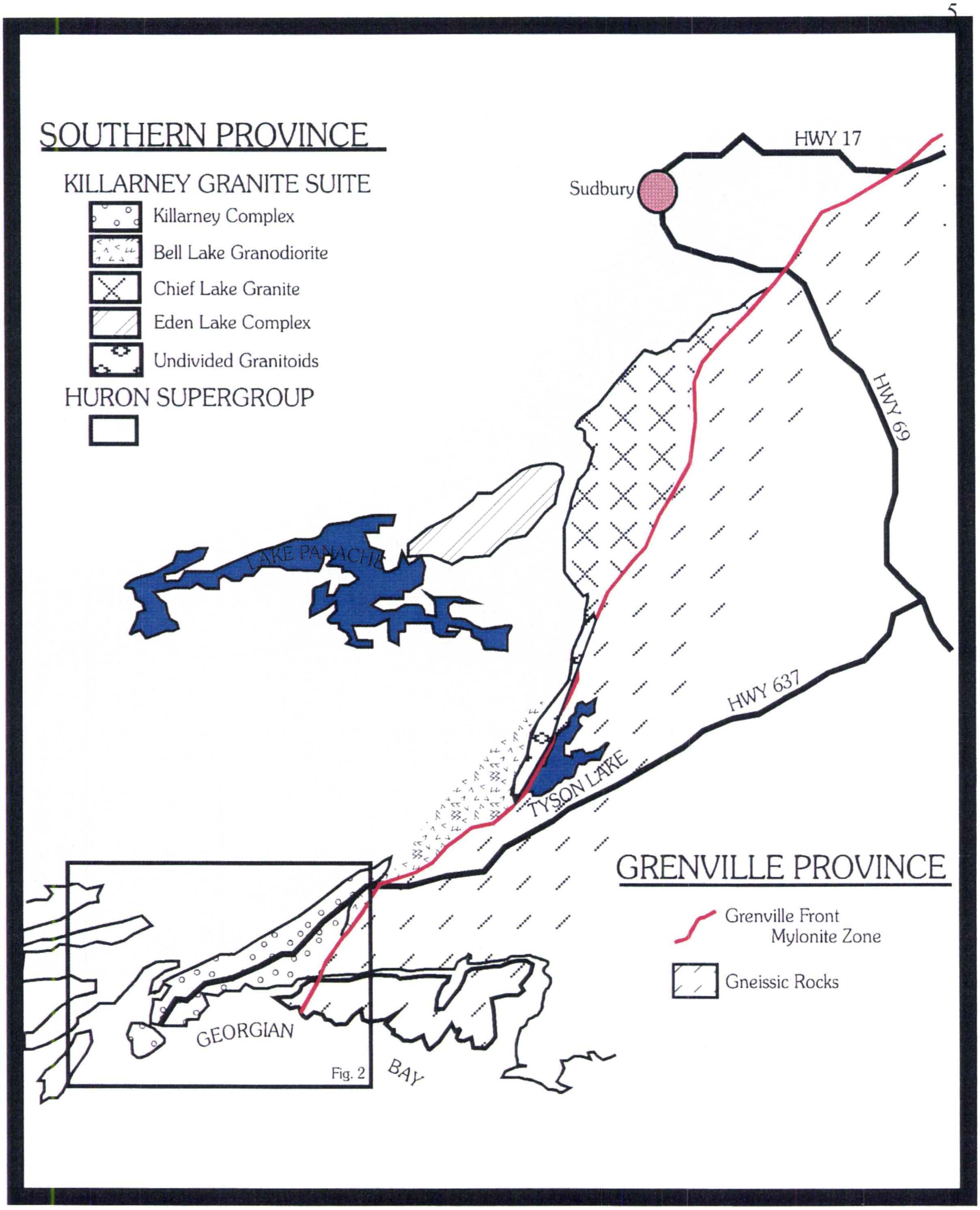

Figure One: Regional Map of Study Area

Shown is the Southern and Grenville Province and locations of Pluton Bodies

Loveridge (1972) have dated the Killarney granite at 1,623 ± 74 Ma using Rb-Sr whole rock isochron methods, which may be a reset date from metamorphism. Van Bremer and Davidson (1988) have recently U-Pb dated the original intrusion of the complex to be 1740 to 1732 Ma. On the north margin of the Killarney complex an intrusive contact is found between it and the Huron Supergroup (figure 2). To the southeast the complex is bounded by the Grenville Front. It is in this part of the complex where greater deformation can be identified. Numerous fractures continue for great lengths, all with an approximate orientation of 230/80. Fan (1995) further studied the fractures and their distribution in which my study areas was located. He also noticed the bands of mylonites and their occurrence in the more deformed southern region. They are usually bounded by faults and range in thickness of a few cms. Mylonites are a form of ductile deformation and occur at depth. They are derived from wall rock and display evidence of flow and reduced grain size; in some cases recrystallization may also occur.

This thesis comprises two study areas approximately six meters square, which are located in the more southern region of this complex, figure 3 and 4, about 500 metres apart. Both areas were drilled to obtain one inch core samples which were analysed later in the lab. All the cores were orientated using a combination of a magnetic and sun compass, such that the magnetic fabric to be measured can be reoriented to define the absolute orientation of the rock body sampled.

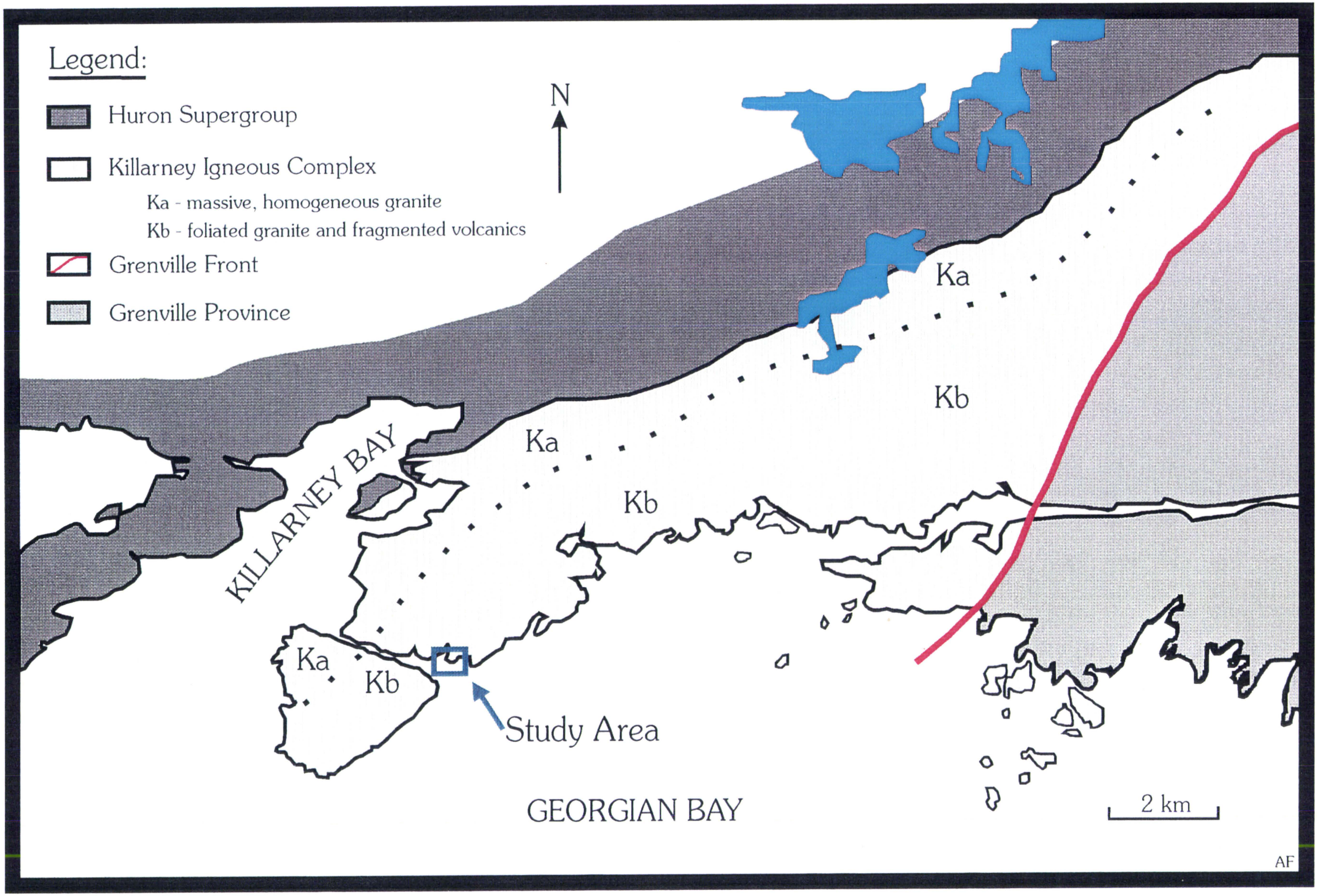

Figure Two: Location of Study Area in the Killarney Igneous Complex

Figure Three:

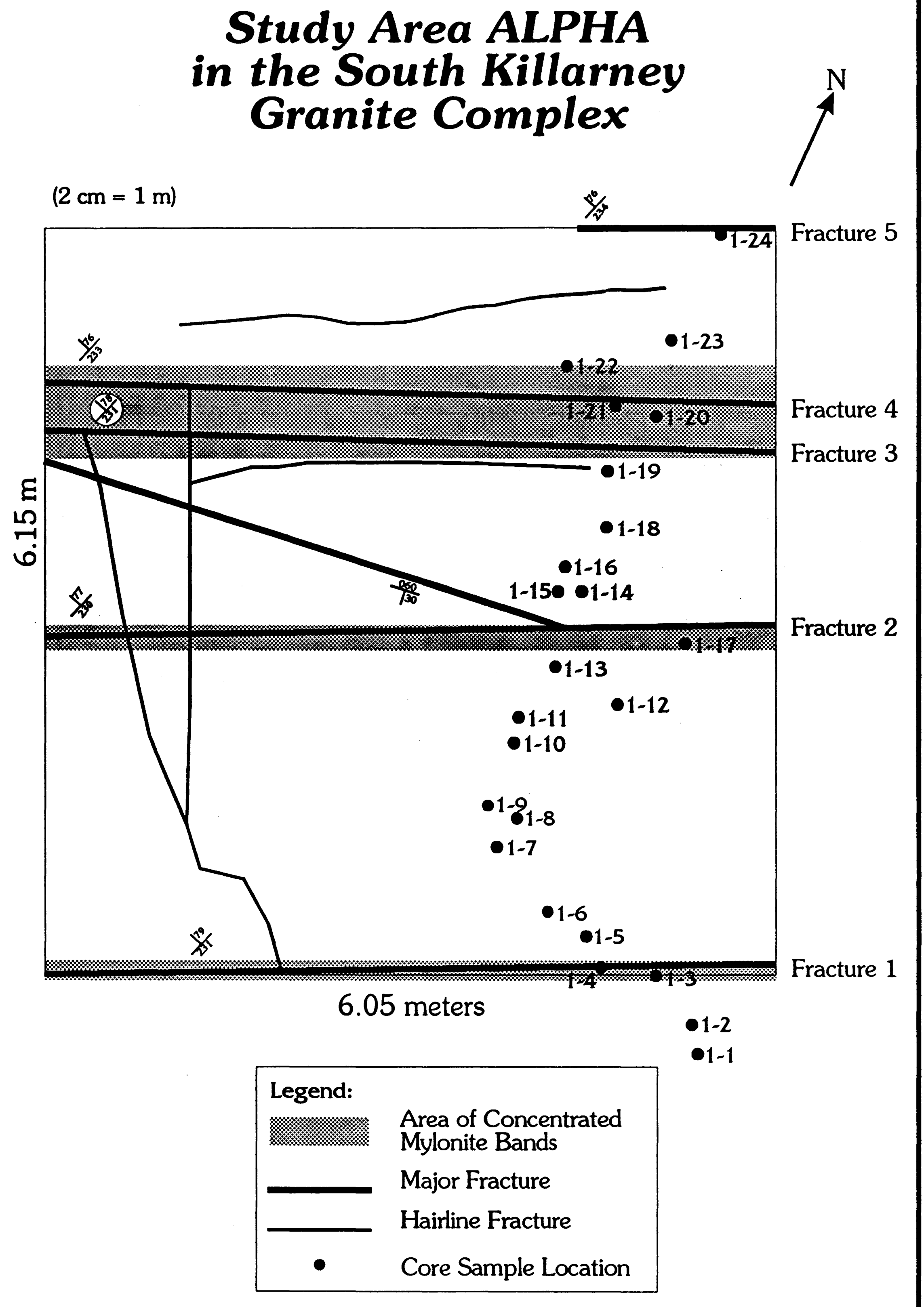

Figure Four:

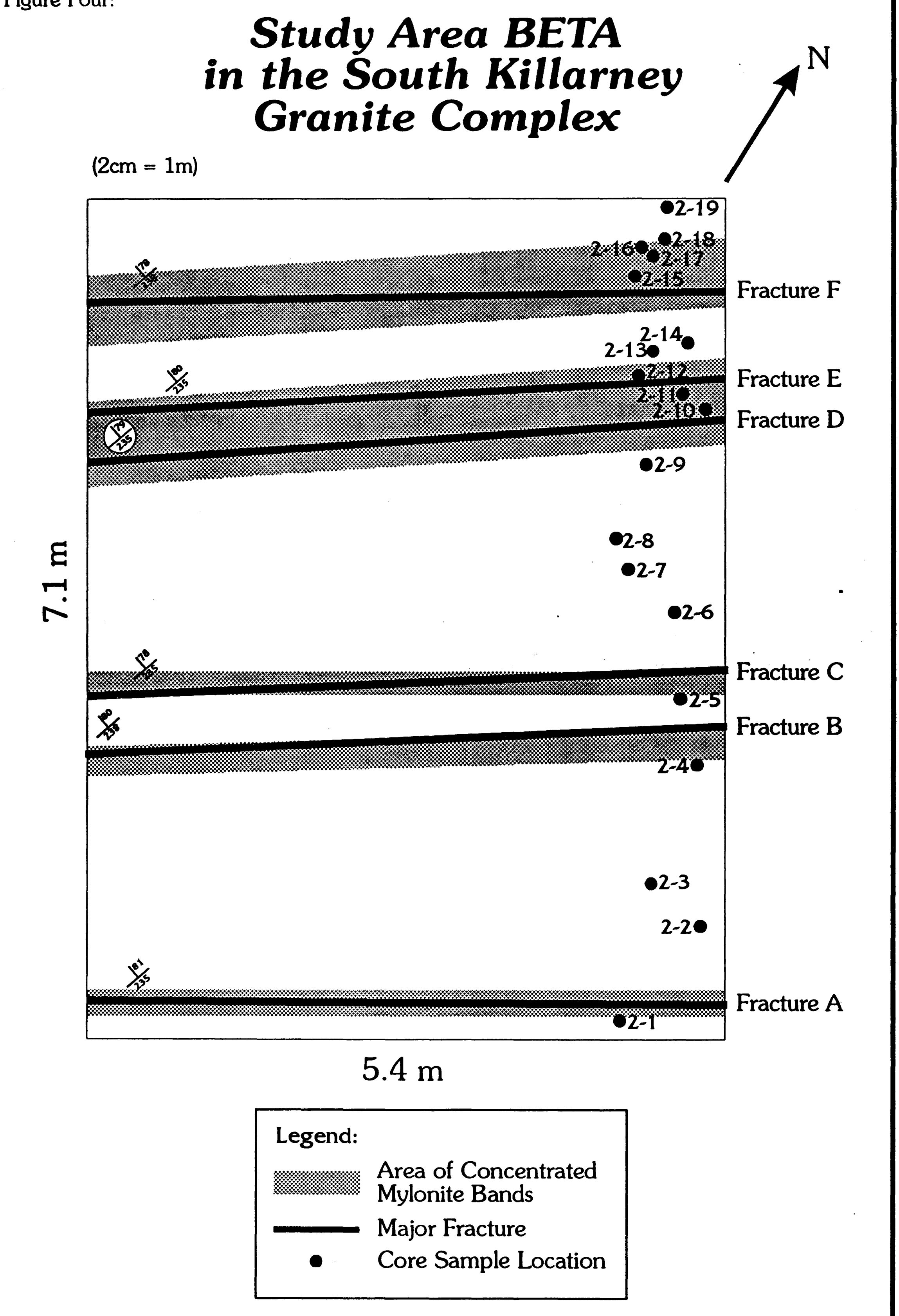
Study Area BETA
in the South Killarney
Granite Complex
(2cm = 1m)
N
2-19
2-18
2-16
2-17
2-15
Fracture F
2-14
2-13
2-12
Fracture E
2-11
2-10
Fracture D
2-9
2-8
2-7
2-6
Fracture C
2-5
Fracture B
2-4
2-3
2-2
Fracture A
2-1
7.1 m
5.4 m
Legend:
Area of Concentrated Mylonite Bands
Major Fracture
Core Sample Location

Method:

Forty - three cores were drilled from two sections in the southern region of the Killarney Igneous Complex, twenty four on ALPHA and nineteen on BETA. They were directly cored from the granitic country rock in areas with high and low intensities of deformation. High intensity deformation was considered to be where the greatest frequency of fractures and mylonties occurred. Back in the lab, fabric, remanence and petrography were measured from all of the cores.

Measurement of Magnetic Fabric:

AMS, anisotropy of magnetic susceptibility, was measured using a Bartington MS2-B with a AMS-BAR program, using nine positions. From these measurements AMS-BAR calculated the direction and intensity of the maximum, intermediate and minimum axes, which can be plotted to show a magnetic plane or ellipsoid. An example of the data which the AMS-BAR program computes, can be seen in Appendix A.

Natural remanent magnetization was measured by using a Molspin Digital Spinner Magnetometer. Once the original fabric and remanence were measured the samples were progressively demagnetized using a Schonstedt GSD-1 Alternating Field Demagnetiser in fields of 5, 15, 20,40, and 50 mT. Both fabric and remanence were again measured after each demagnetizing step. Repeating of the remanence measurements were conducted to examine for any possibility of remanence overprinting. Fabric work by Park et al (1988) has suggested that using alternating field methods may aid in determining any domain changes in the fabric.

Finally each specimen was subjected to ARM in a 100 mT alternating field with a 0.6 T bias field. King et al (1982) have shown that ARM/X is related to magnetic grain size, but is only sensitive to fine grain sizes.

Measurement of Petrological Fabric:

After cutting the cores to the required volume for the magnetic fabric measurements, most cores had sufficient pieces remaining to have thin sections produced. They were taken above the long axis perpendicular to the core which was to be used for magnetic measurements. Due to the overall reduction of grain size, photographs were taken to magnify the whole area of the thin sections to determine a regional fabric. Petrological fabric was determined using a microscope under crossed and regular polarized light at 40X and the photographs mentioned above. Polished thin sections were not obtained to distinguish between the magnetite and hematite. This was performed by Wiacek (1989) on samples from the same area and I have assumed a similar mineralogy.

Additional grain properties, such as the maximum axis length and its orientation, were measured on selected samples using an Image Analyzer and the program Northern Exposure. This technique allows the user to define which type of grains are to be included for the statistics. The program utilizes shades of greens and reds to define the species in the thin sections, making if difficult to differentiate the minerals with similar light properties. Opaques were black, biotites red and the more transparent minerals are green. Magnetite, being opaque and thus black on the view screen, was the easiest mineral to define. Individual biotites were traced on the screen, which means that only the larger grains have been measured.

For the minerals which were investigated through the above method, a count was taken to determine their approximate percentage in the sample. Data which was collected by this method was only useful in the dimension of which the thin section was cut; therefore did not weigh heavily on the results when referring to the grain shape and its preferred orientation.

Results:

Magnetic Fabric:

The AMS calculation provides estimates of the bulk susceptibility, percent anisotropy, orientation and intensity of maximum, intermediate and minimum axes of the AMS ellipsoid. The bulk susceptibility was plotted to determine if there was a change in magnetic mineralogy across the study areas (figures 5,7). Although the average susceptibilities for the study areas are high, no major change can be seen other than in samples 14, 15 and 17 in Alpha and samples 15, 16a, 16b and 17 in Beta. When the percent anisotropy is plotted (figures 6,8), a similar situation occurs, such that there is no significant change across the study area. Although, there are changes such as the increased anisotropy of 14 and 15 in Alpha and of 16a, 16b and 17 in Beta. Study area Alpha is not as intense as Beta, but has a consistent anisotropy, within ten percent, throughout the samples collected. Sample 14 and 15 in Alpha do experience a higher anisotropy relative to the samples collected in this area, but do not increase as dramatically as 16a, 16b and 17 in the Beta group. A relationship is therefore seen between the very low bulk susceptibilities and high anisotropies in both study areas.

AMS data further defines the maximum (k1), intermediate (k2) and minimum (k3) susceptibility axis which were plotted using Rockware STEREONET, (figures 9 through 17). A great circle was calculated using the k2 and k3 axis which indicates

Figure Five:

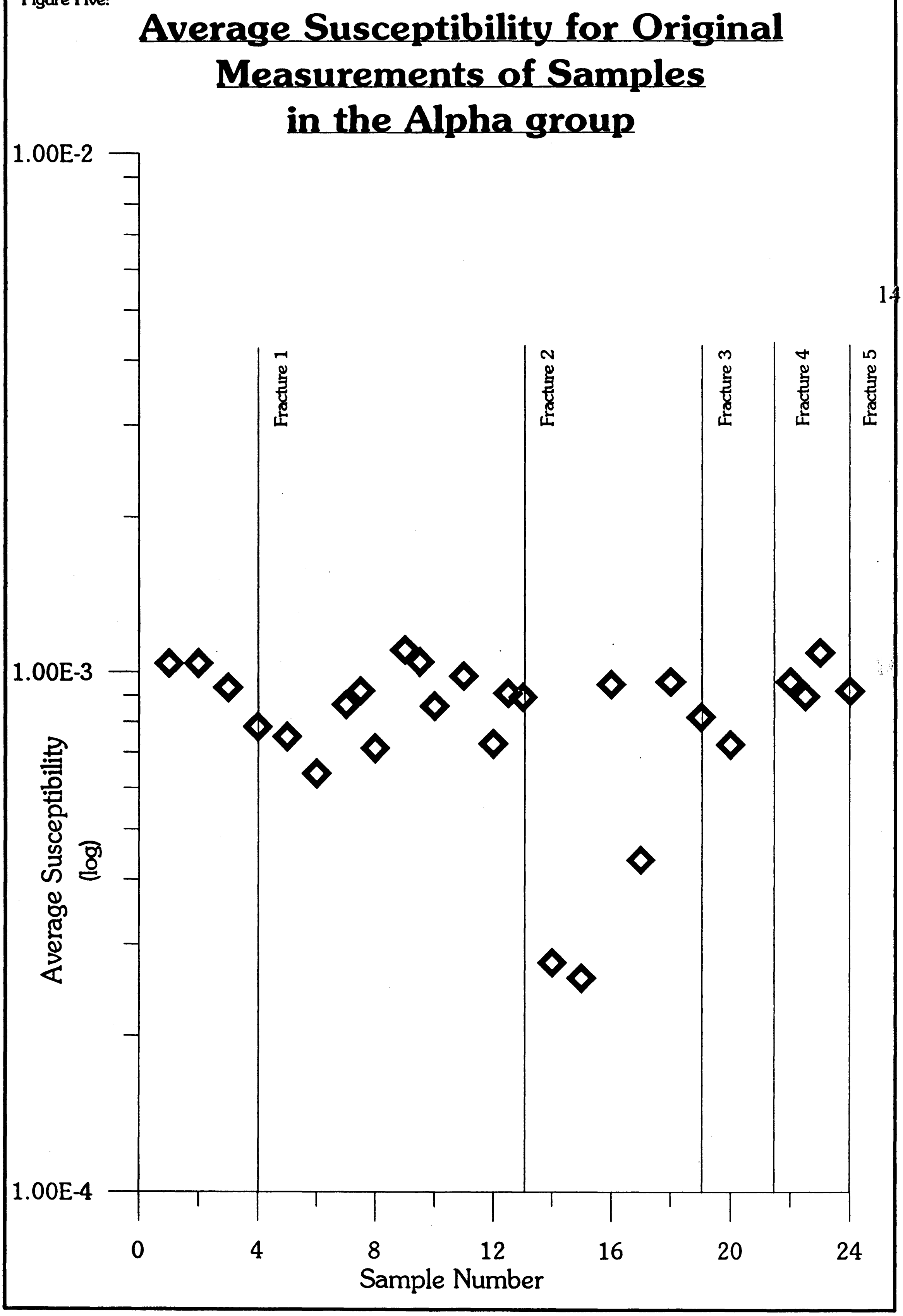
Average Susceptibility for Original Measurements of Samples in the Alpha group
1.00E-2
1.00E-3
1.00E-4
Average Susceptibility (log)
Fracture 1
Fracture 2
Fracture 3
Fracture 4
Fracture 5
0
4
8
12
16
20
24
Sample Number

Figure Six:

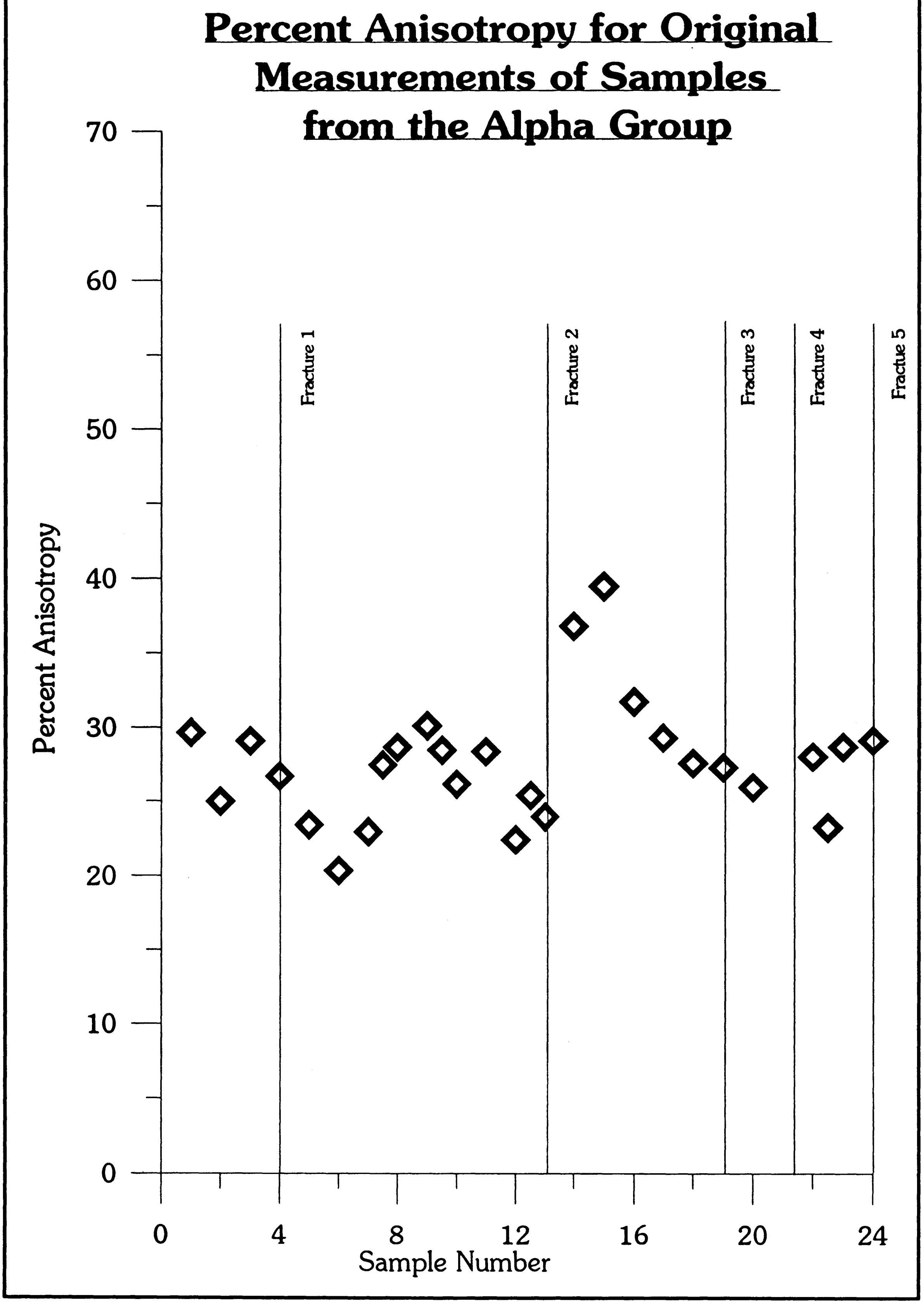
Percent Anisotropy for Original Measurements of Samples from the Alpha Group
Percent Anisotropy
Sample Number
0
10
20
30
40
50
60
70
0
4
8
12
16
20
24
Fracture 1
Fracture 2
Fracture 3
Fracture 4
Fractue 5

Figure Seven:

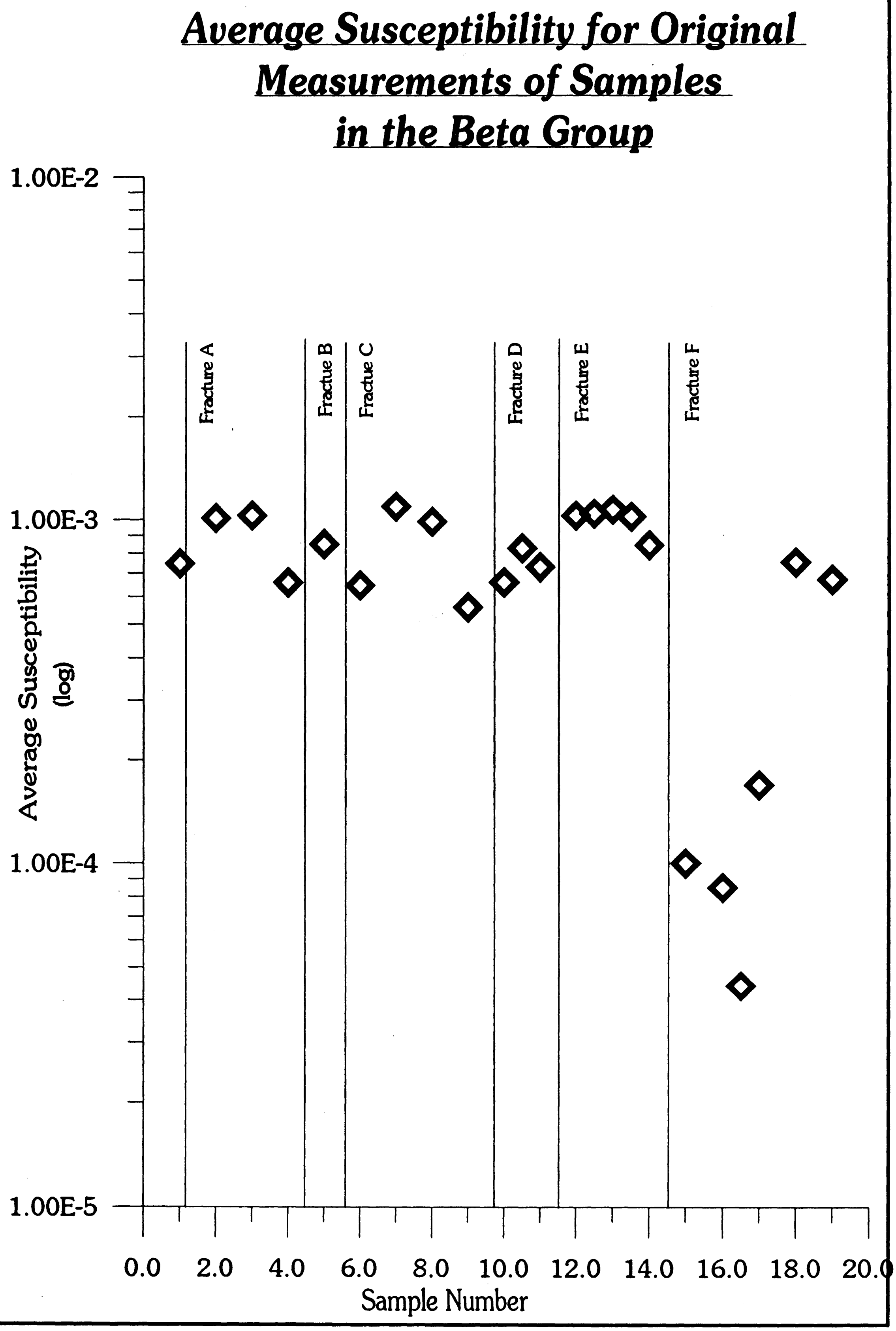

Figure Eight:

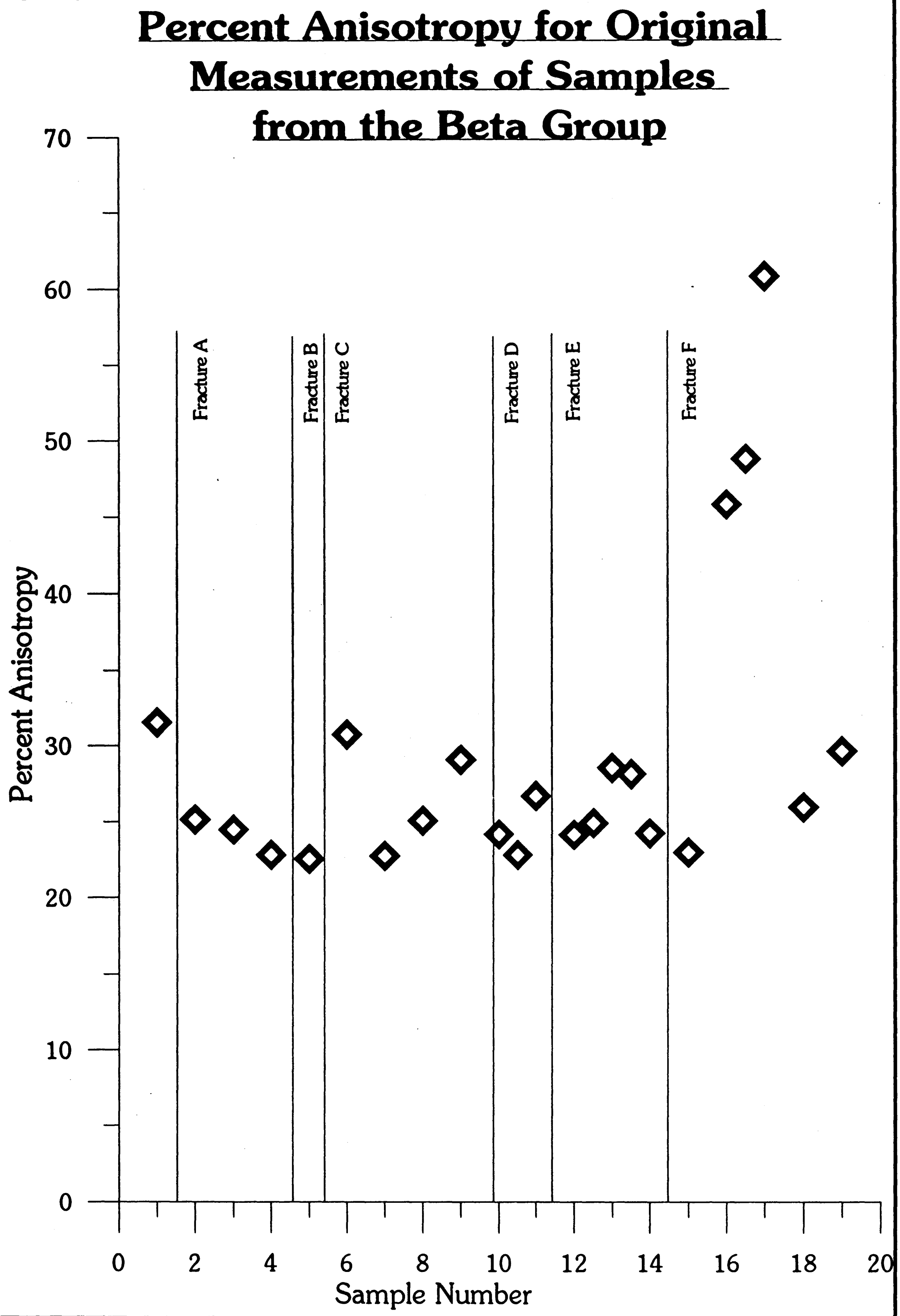

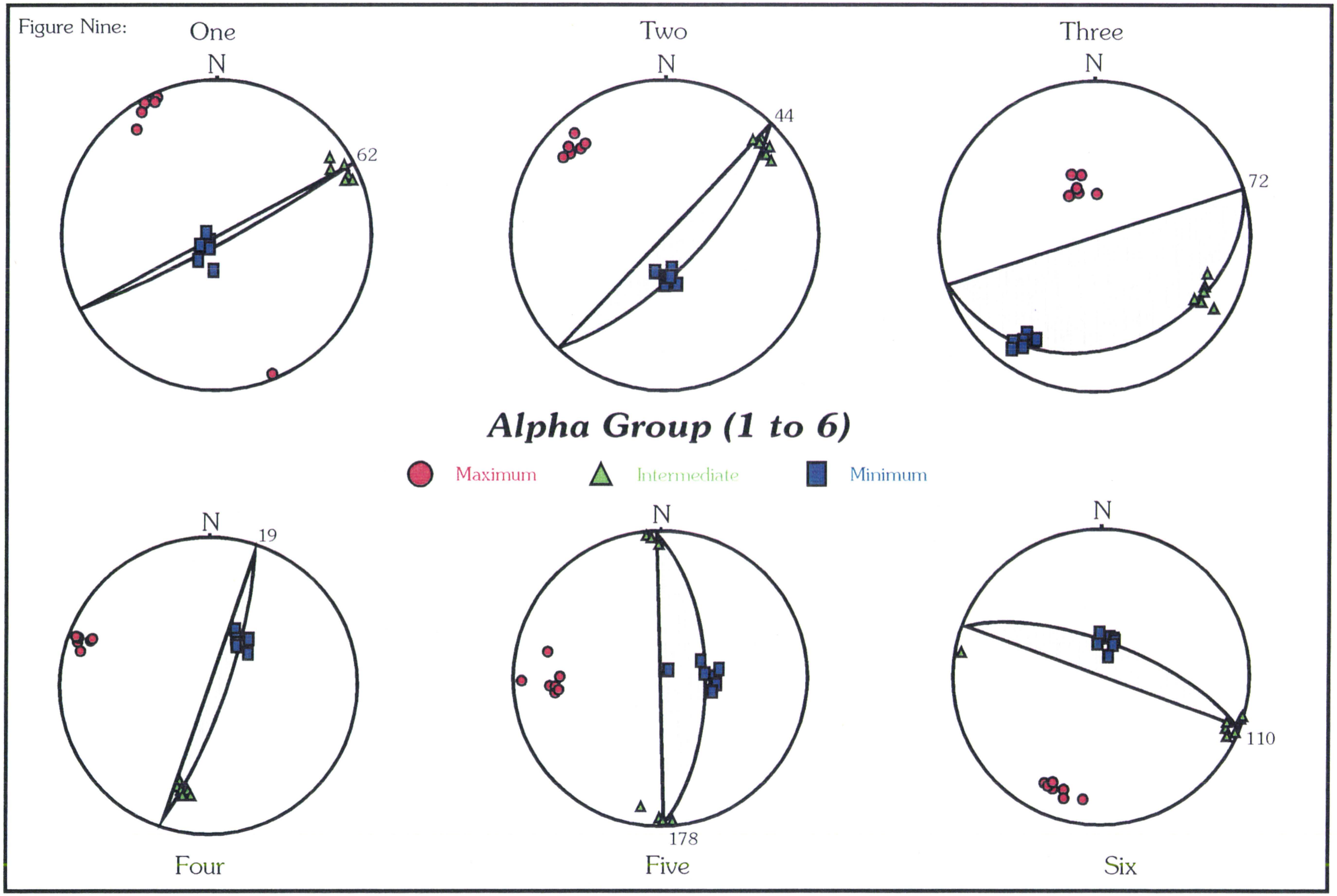
Figure Nine:
One
N
62
Two
N
44
Three
N
72
Alpha Group (1 to 6)
Maximum
Intermediate
Minimum
N
19
Four
N
178
Five
N
110
Six

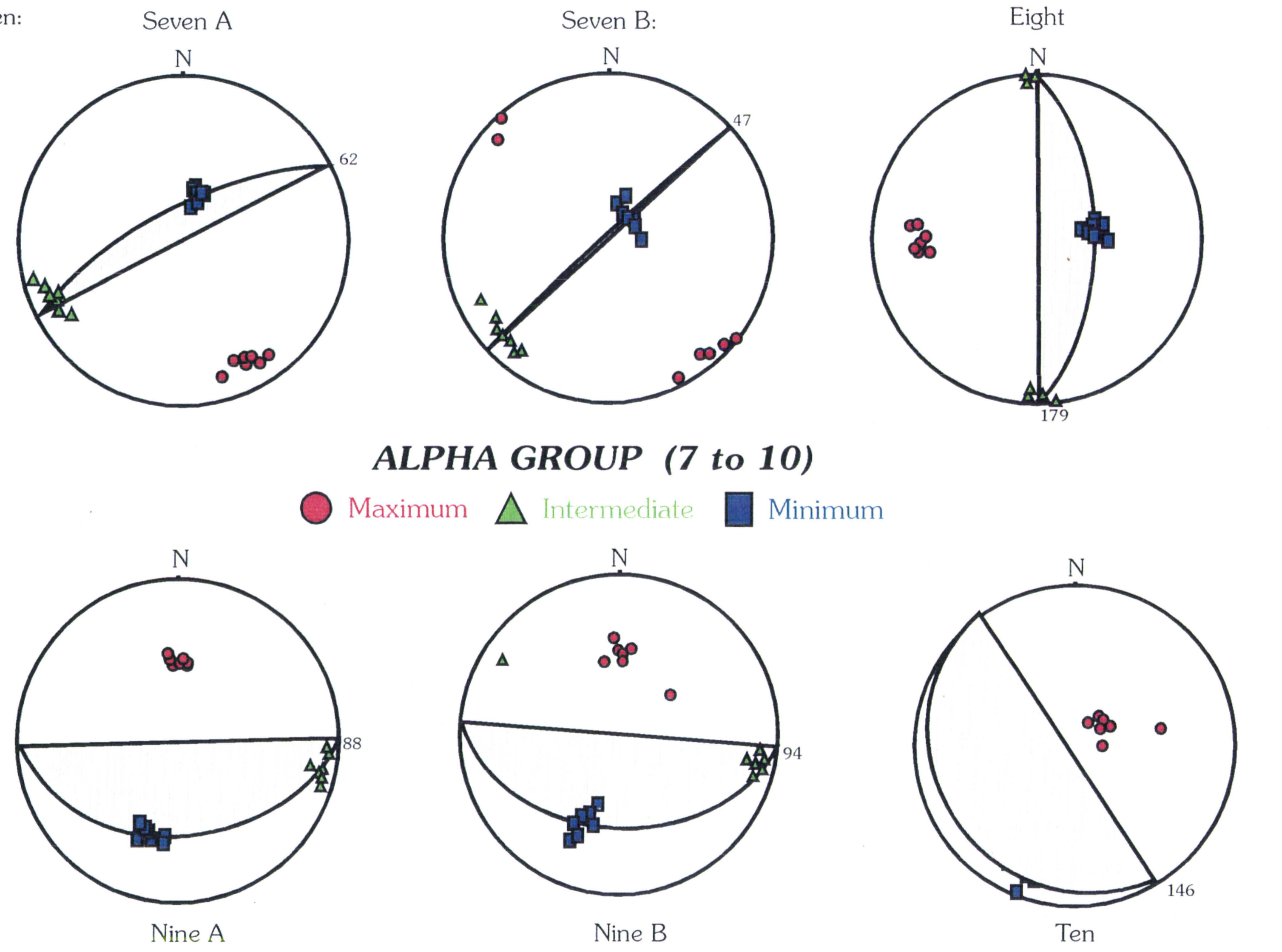
Seven A
N
62
Seven B:
N
47
Eight
N
179
ALPHA GROUP (7 to 10)
Maximum
Intermediate
Minimum
N
88
Nine A
N
94
Nine B
N
146
Ten

Figure Ten:

Figure Eleven:

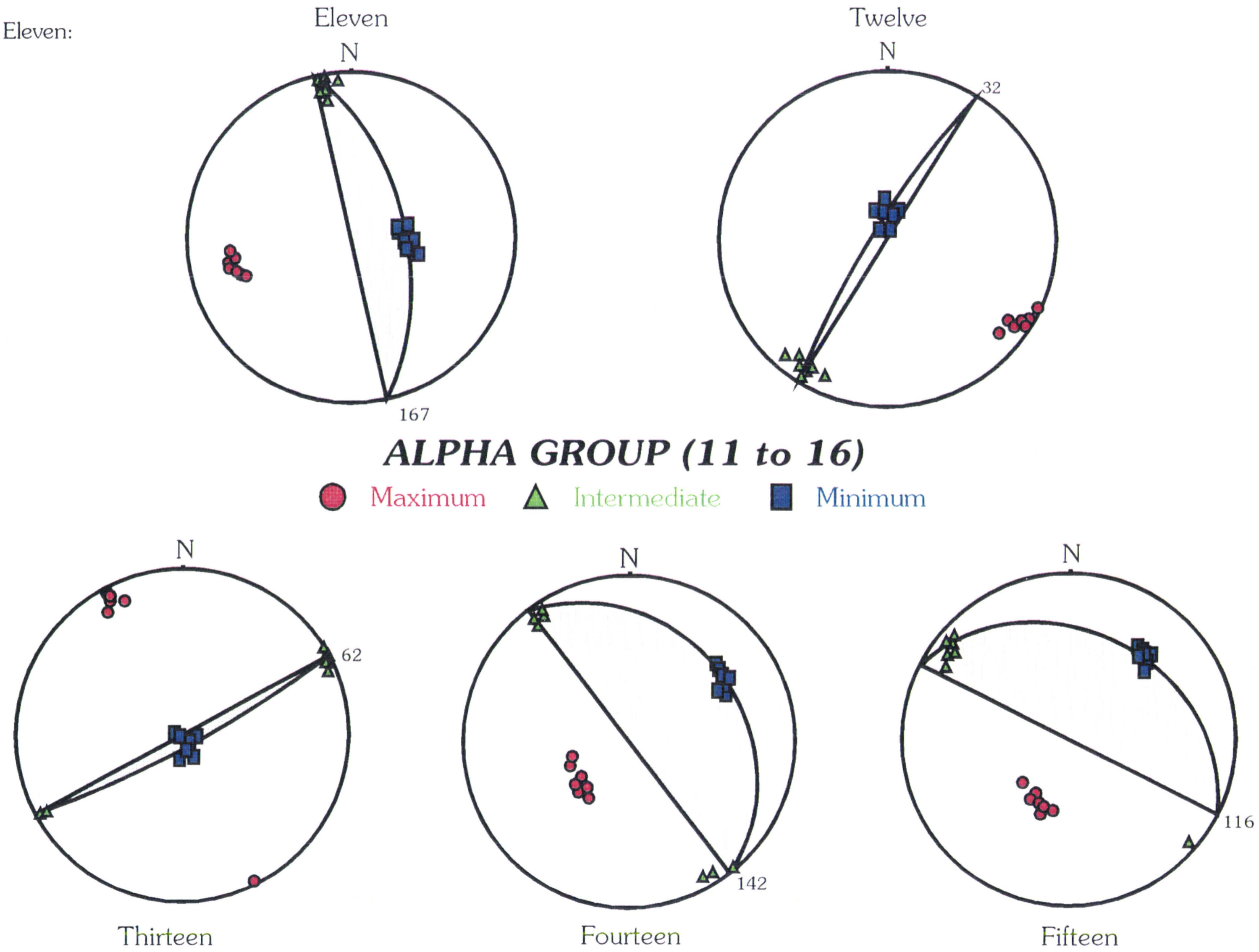

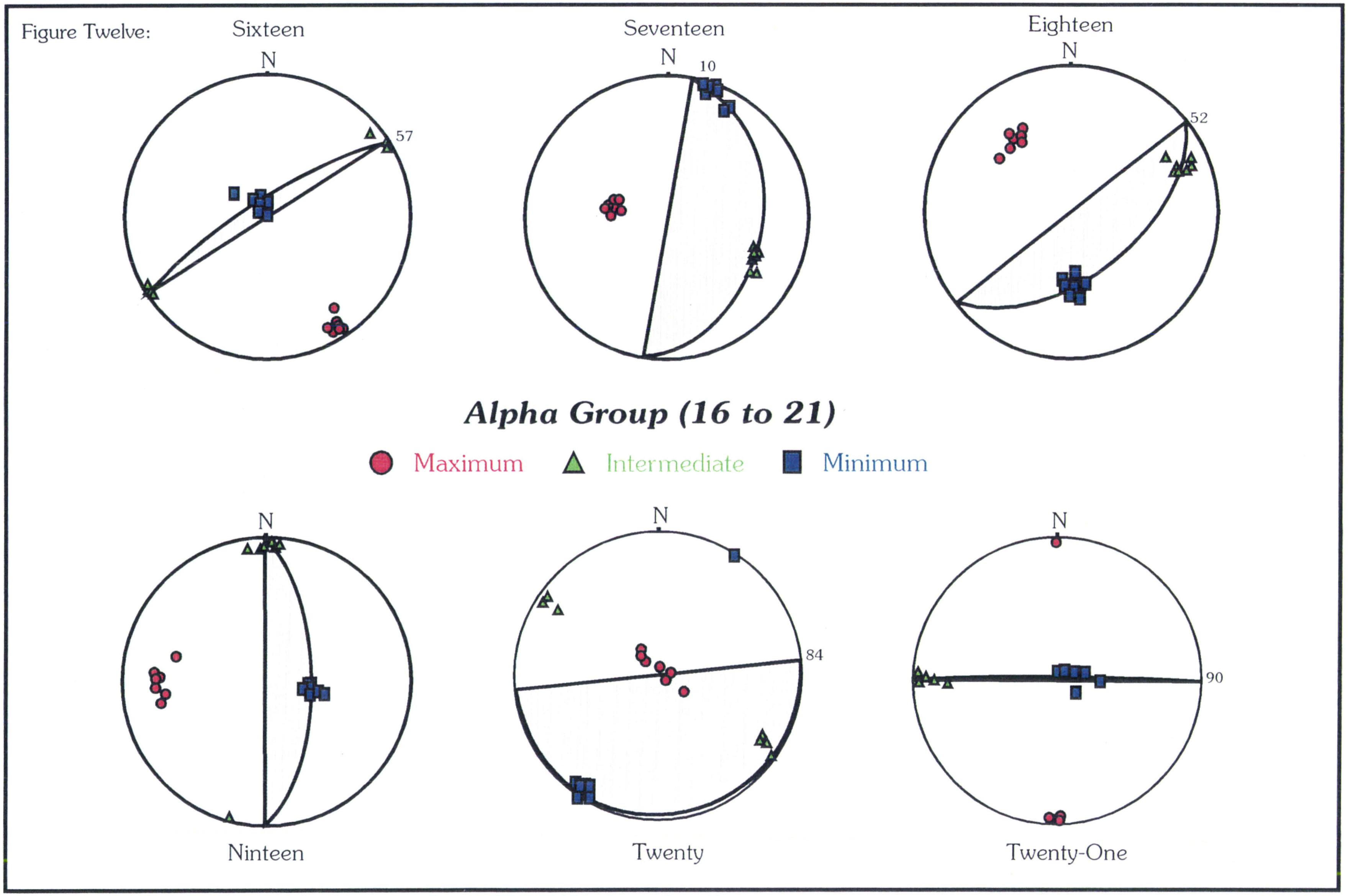

Figure Twelve:

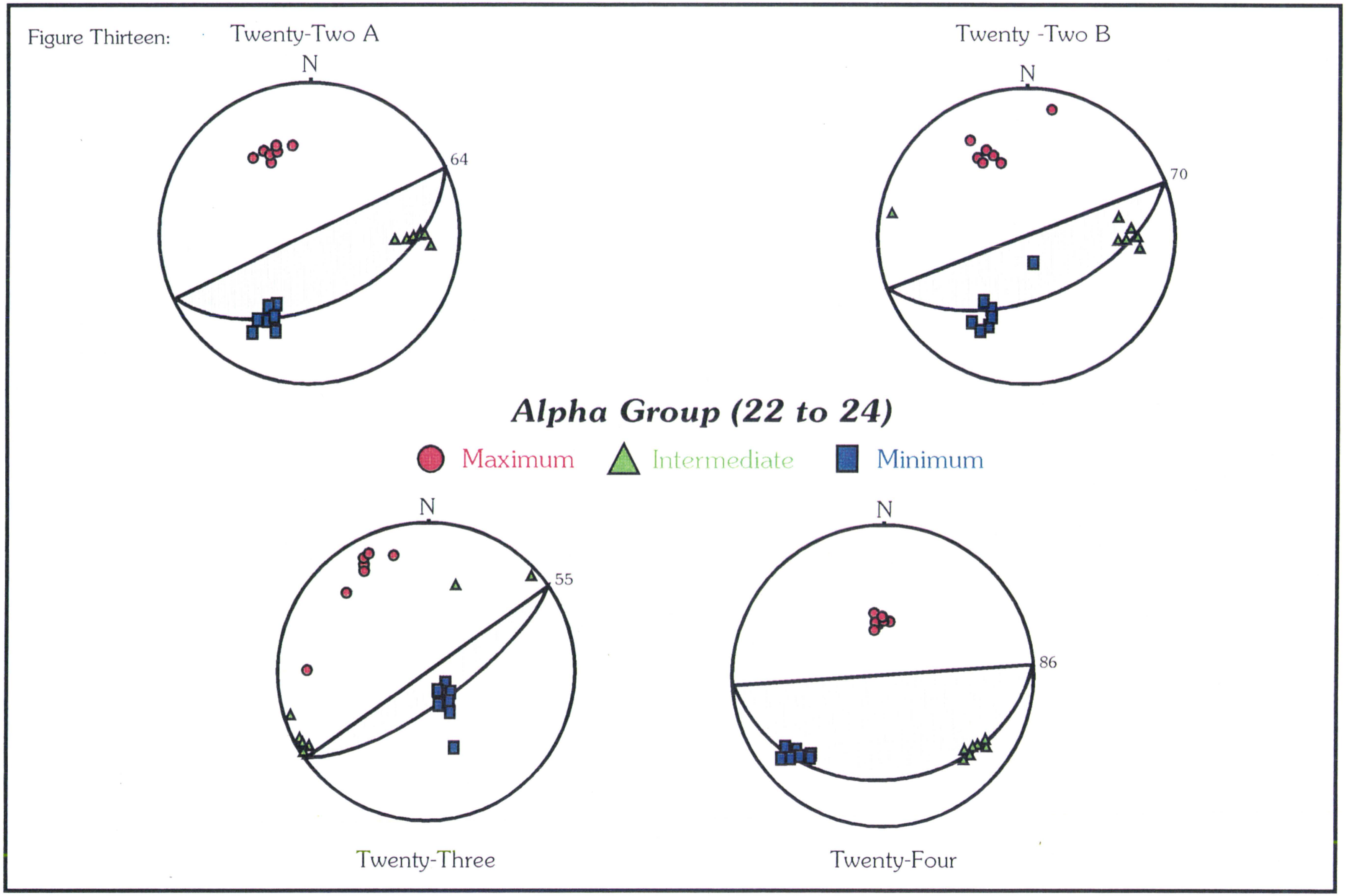
Figure Thirteen:
Twenty-Two A
N
64
Twenty -Two B
N
70
Alpha Group (22 to 24)
Maximum
Intermediate
Minimum
N
55
Twenty-Three
N
86
Twenty-Four

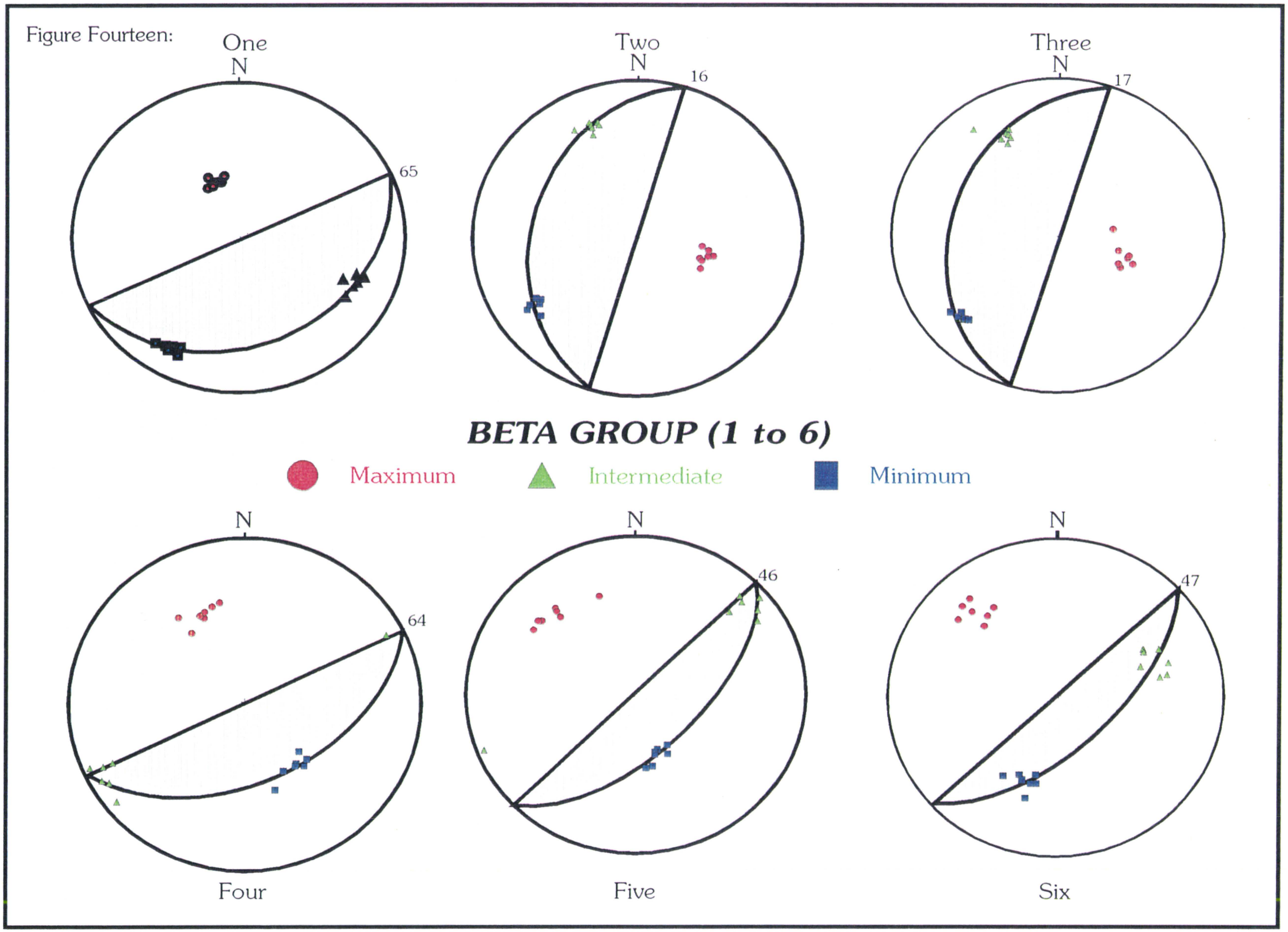

Figure Fourteen:

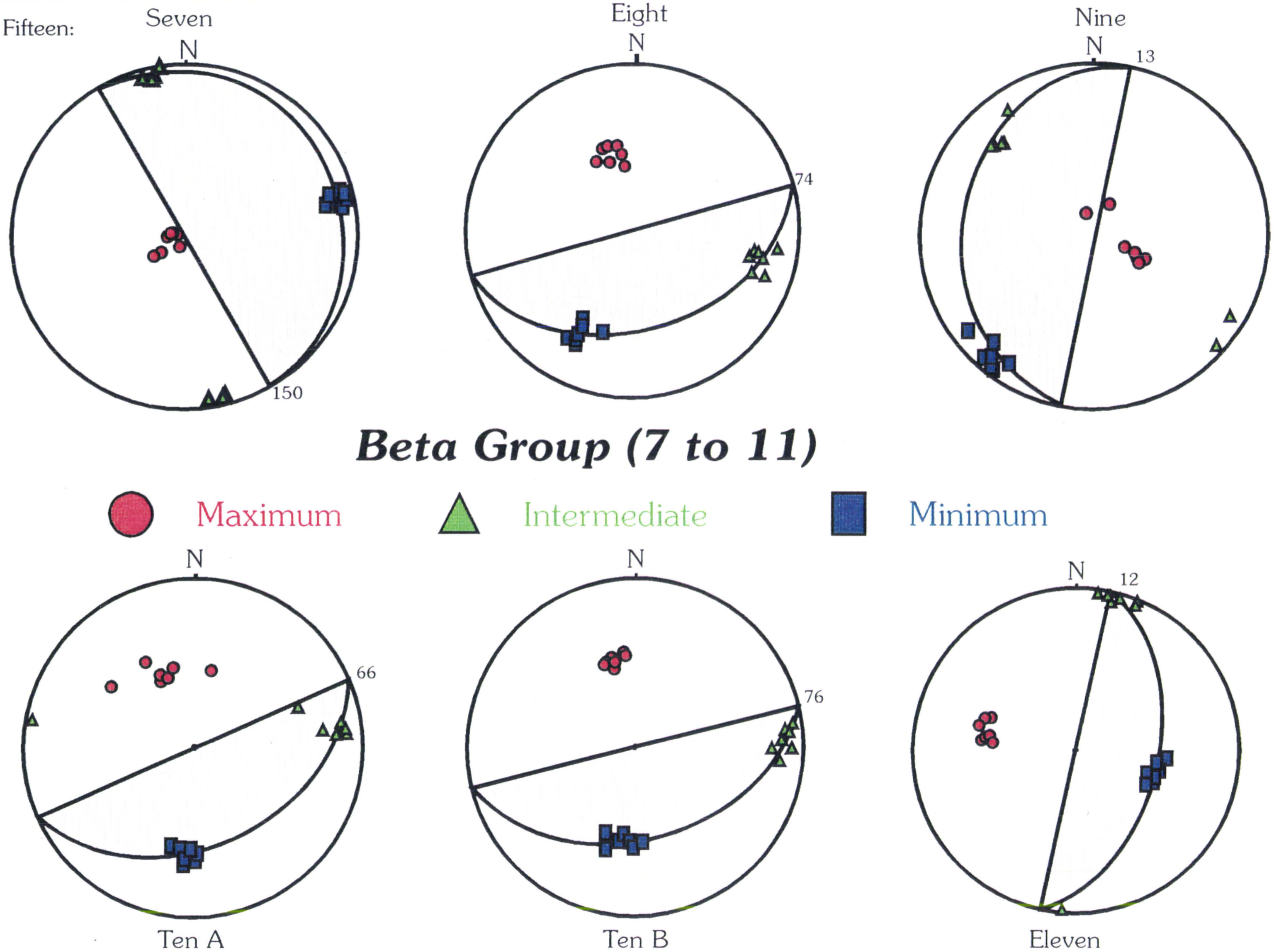

Figure Fifteen:

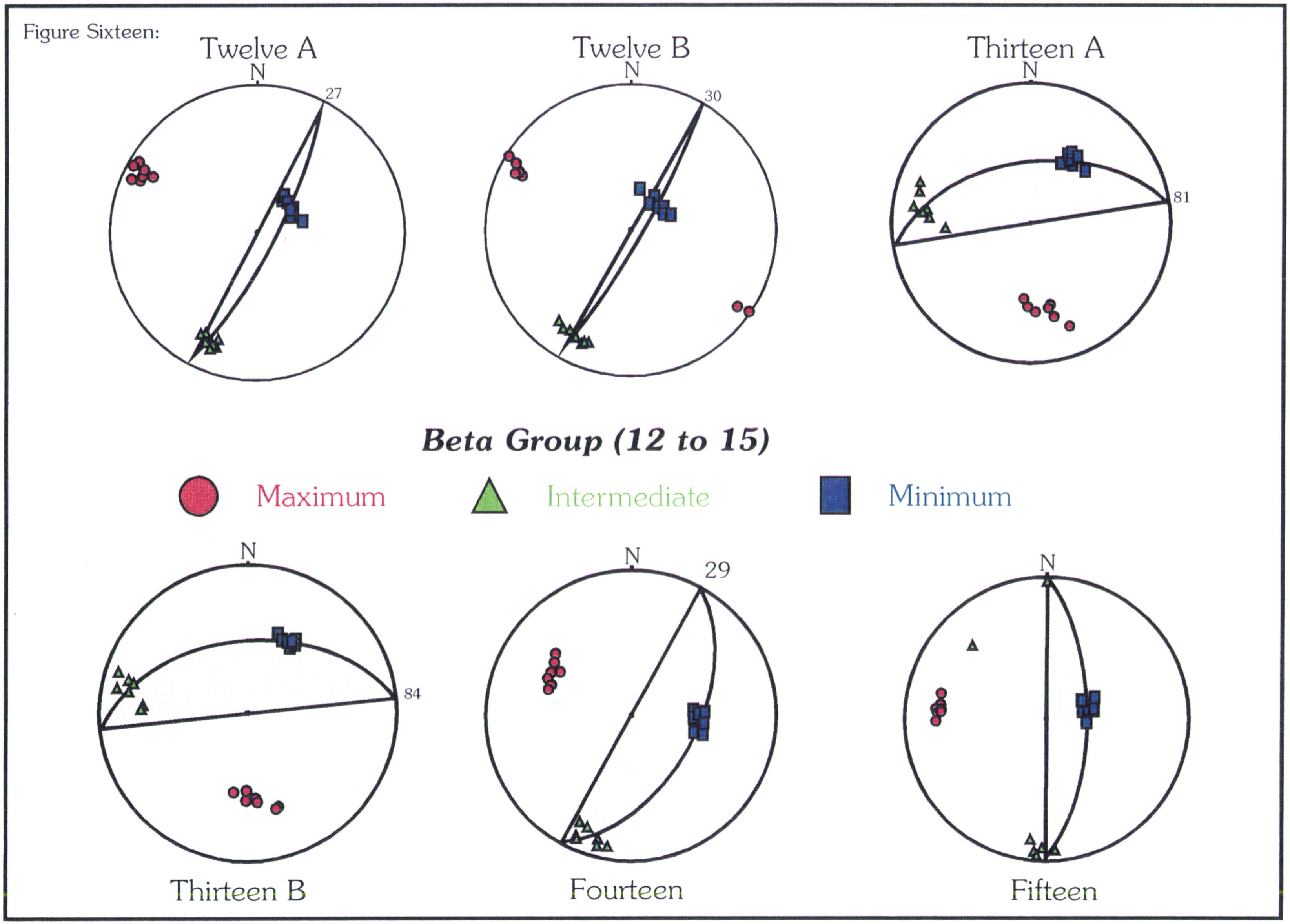

Figure Sixteen:

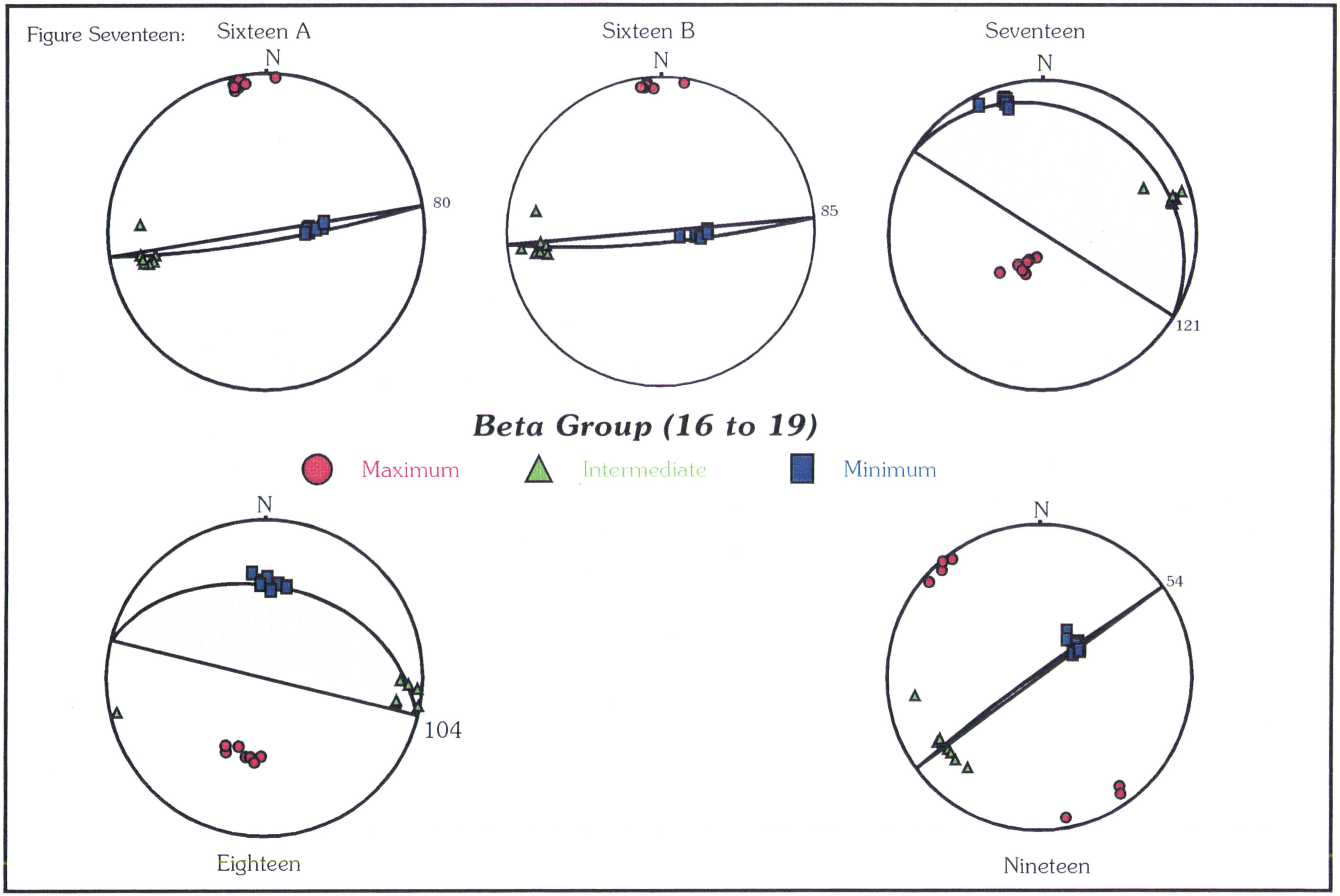
Figure Seventeen:
Sixteen A
N
80
Sixteen B
N
85
Seventeen
N
121
Beta Group (16 to 19)
Maximum
Intermediate
Minimum
N
104
Eighteen
N
54
Nineteen

the foliation plane of the magnetic fabric. k1, plotted on the same stereonet, represents the magnetic lineation indicating the orientation of the maximum axis relative to the deformation or magmatic flow. The magnetic foliation planes were then shaded to give a better understanding of the dip of this plane. It is clear from the series of stereonets for both sampled areas, Alpha and Beta, that there are preferred orientations for the foliations and lineations of the magnetic fabric depending on the intensity of deformation.

Further utilizing the AMS data, the geometry of the magnetic ellipsoid can be determined. Plotting k1/k2 (inverse P3), which describes the magnetic lineation, versus k3/k2 (P1), which describes the magnetic foliation, can give some indication of whether the magnetic ellipse is oblate or prolate (figures 18,19). Alpha and Beta study areas indicate similar magnetic ellipsoid shapes, which would be expected. Both study areas indicate a relatively prolate magnetic ellipsoid, but some samples are more defined in the Beta group. By distinguishing the preferred shape of the magnetic ellipse, the type of interaction between magnetically interacting grains may be determined.

Remanence:

Natural remanet magnetisation is plotted in three dimensional space according to its sample number. Both down line and profile perspectives are shown to indicate the north and south trends (profile) and the east and west trends (down line) seen in

Figure Eighteen:

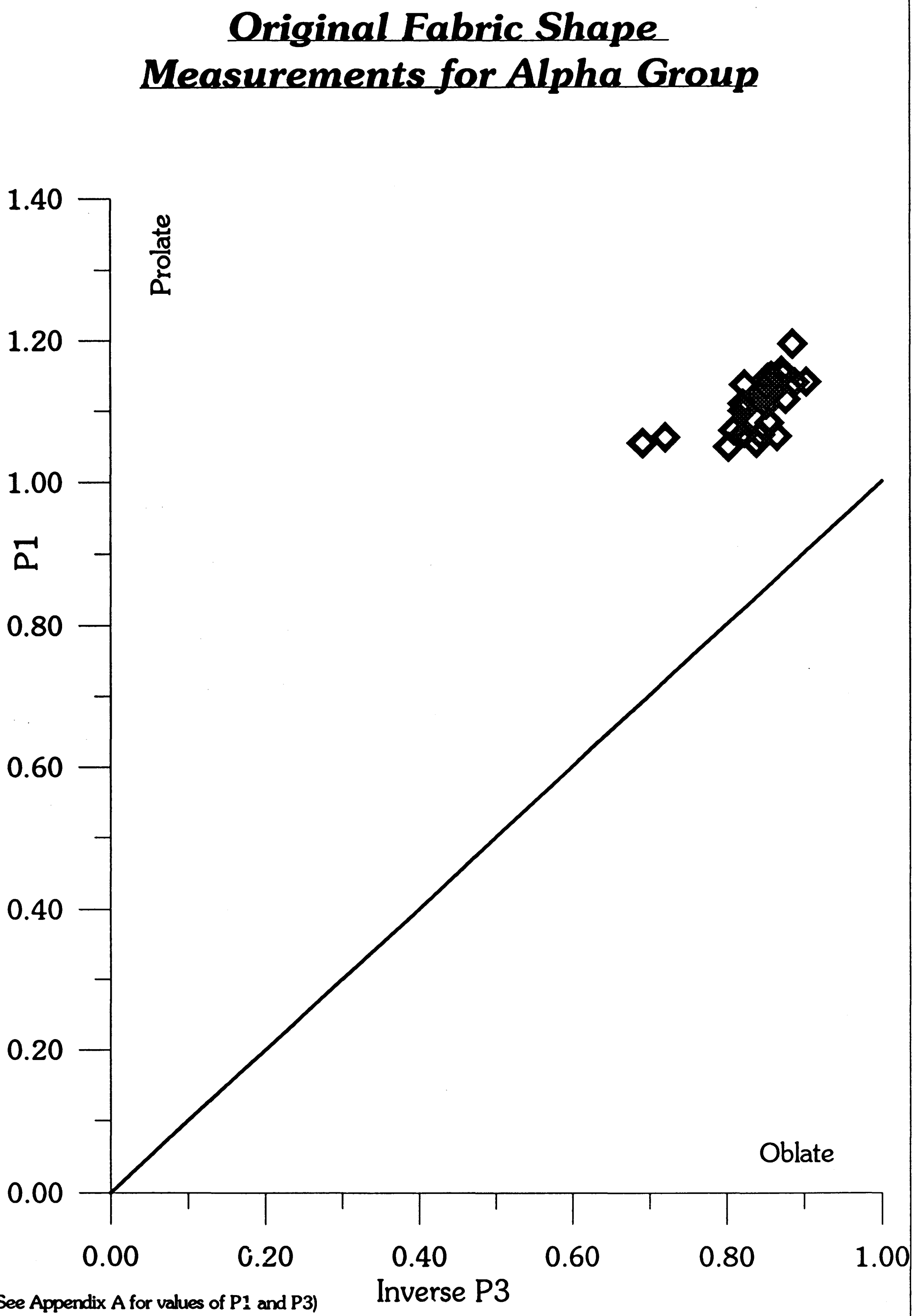

(See Appendix A for values of P1 and P3)

Figure Nineteen:

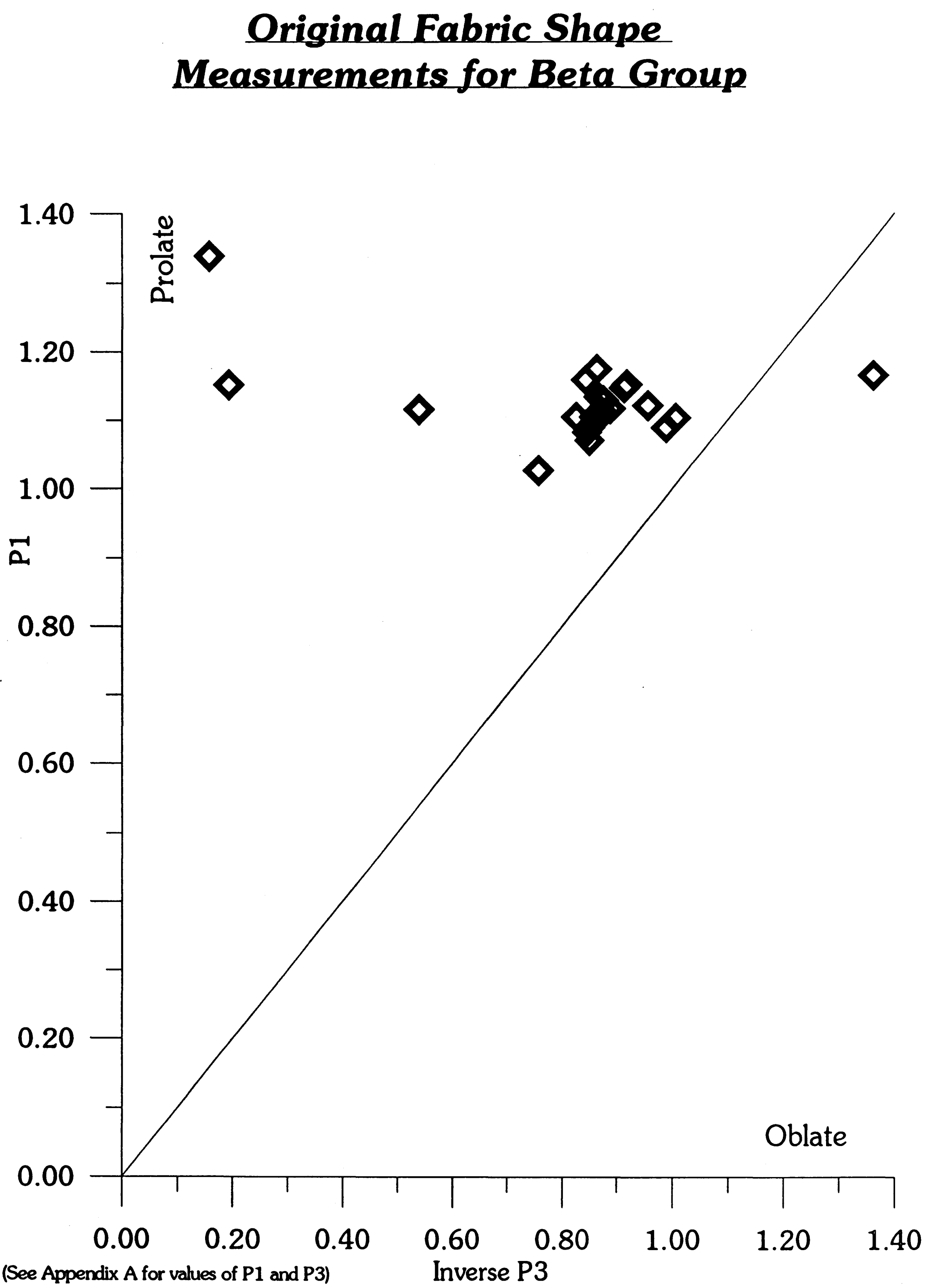

(See Appendix A for values of P1 and P3)

Figure Twenty:

ALPHA - NRM Fabric Orientations

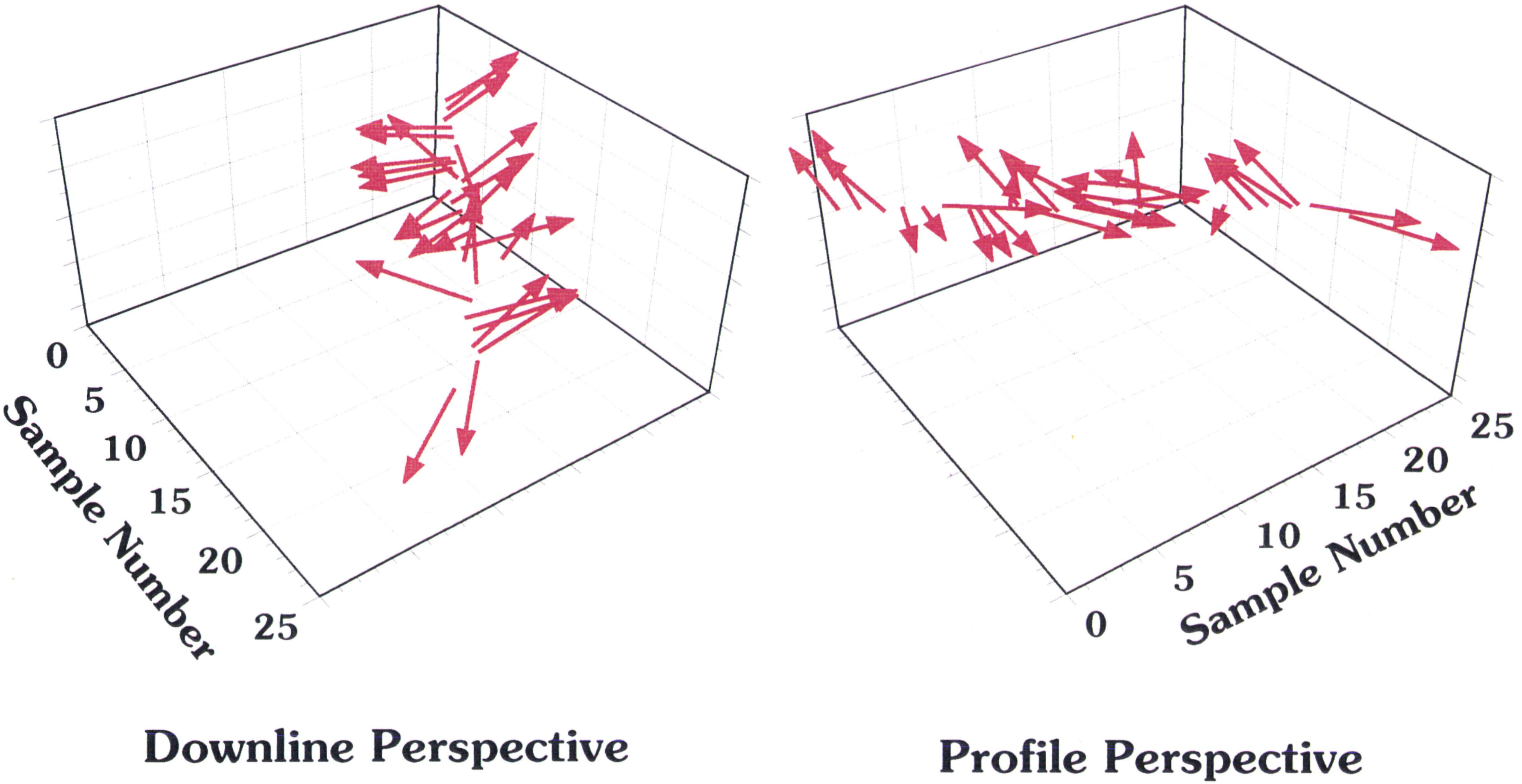

Figure Twenty -One:

BETA - NRM Fabric Orientations

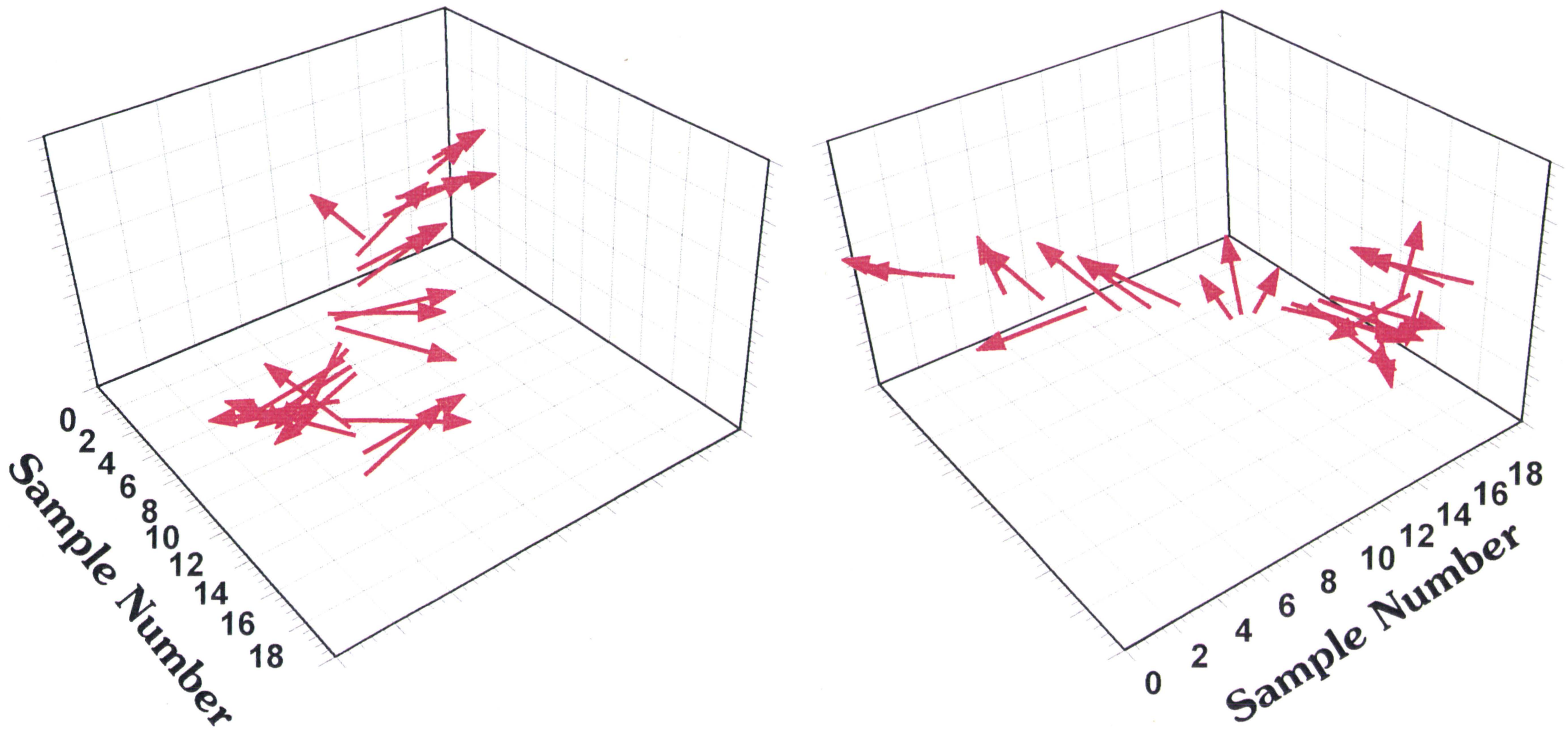

Downline Perspective

Profile Perspective

Figure Twenty-Two:

ARM/ X verses Sample Number

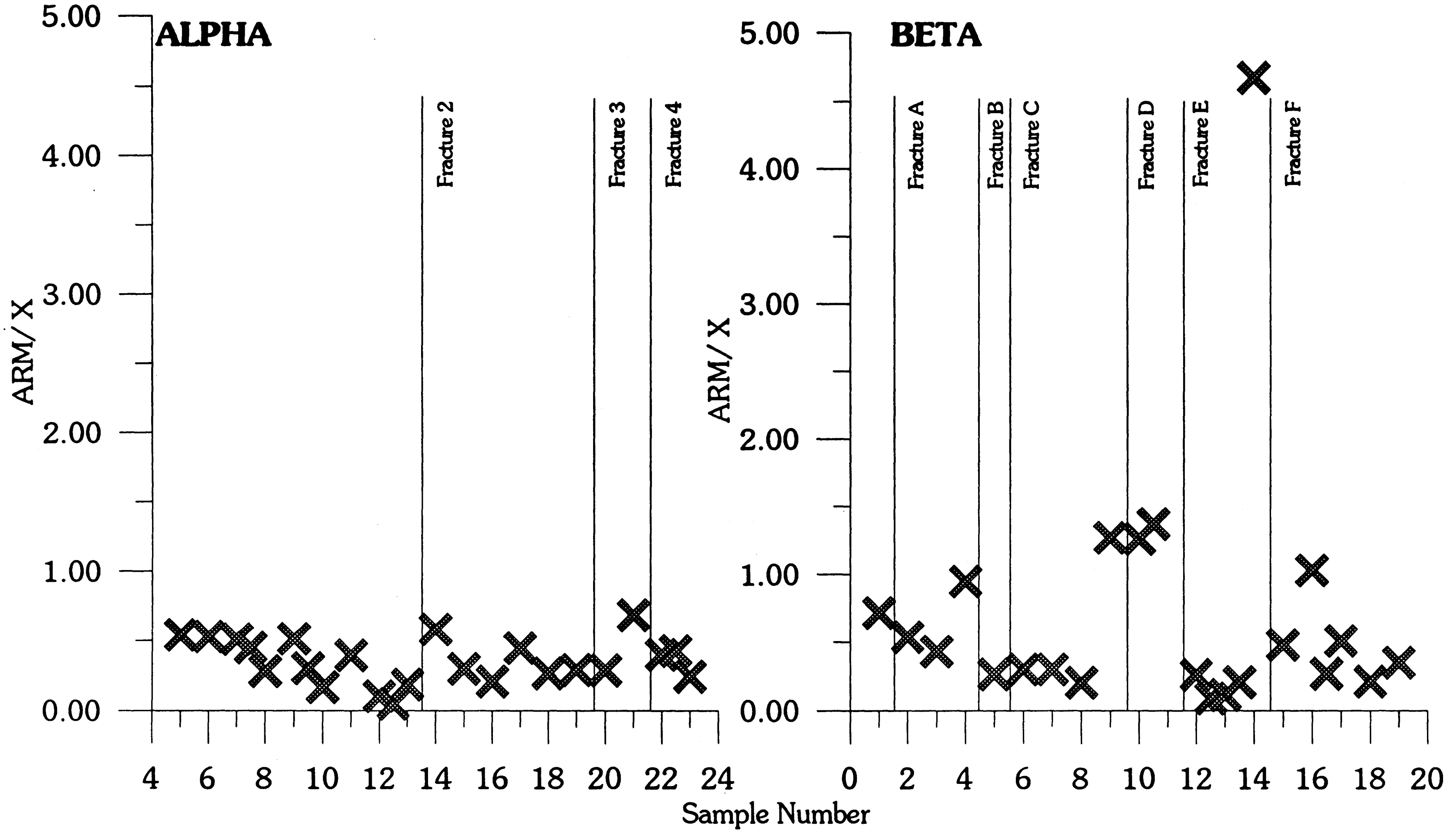

figures 20, 21. This data was further used to determine a relative grain size by plotting the sample number versus the ARM/X, indicated in figure 22. An inverse relationship between grain size and ARM/X indicates that the higher the ARM/X value the finer the grain size present in the sample.

The samples were progressively demagnetised and the measured bulk susceptibility (figures 23,24), percent anisotropy (figures 25,26) and k1, k2 and k3 axis were plotted with the original data measured, figures 9 through 17. Bulk susceptibility again showed no change in the magnetic mineralogy across the study areas. In the Alpha and Beta group the percent anisotropy does not show a significant variance either once any remanence has been removed. If there was remanence in the samples, it would probably be revealed in the plotting of the magnetic foliation and lineation, figures 9 to 16. Most of the samples did not demonstrate any change in their orientation of lineation and foliation. Any variance in the orientation of the remanence would be indicated by the movement of the axes on the stereonets.

Petrological Fabric:

The petrological preferred orientation fabric was mostly determined with the use of the photographs, examples are shown in figures 27 to 33. This method allowed the visualization of the entire thin section to determine if the larger grains were randomly distributed or not. Some thin sections indicate a greater alignment of

Figure Twenty-Three:

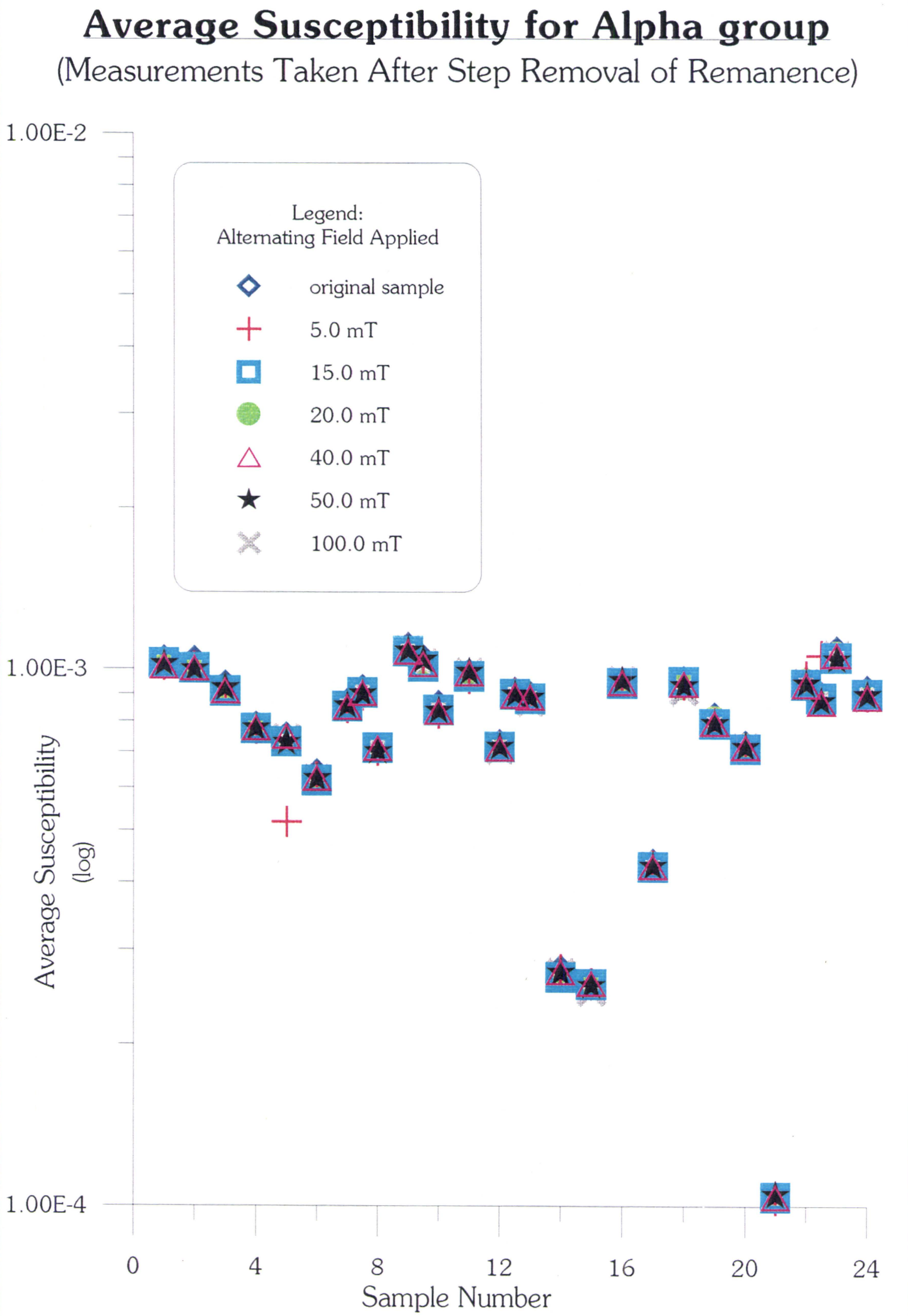

Figure Twenty-Four:

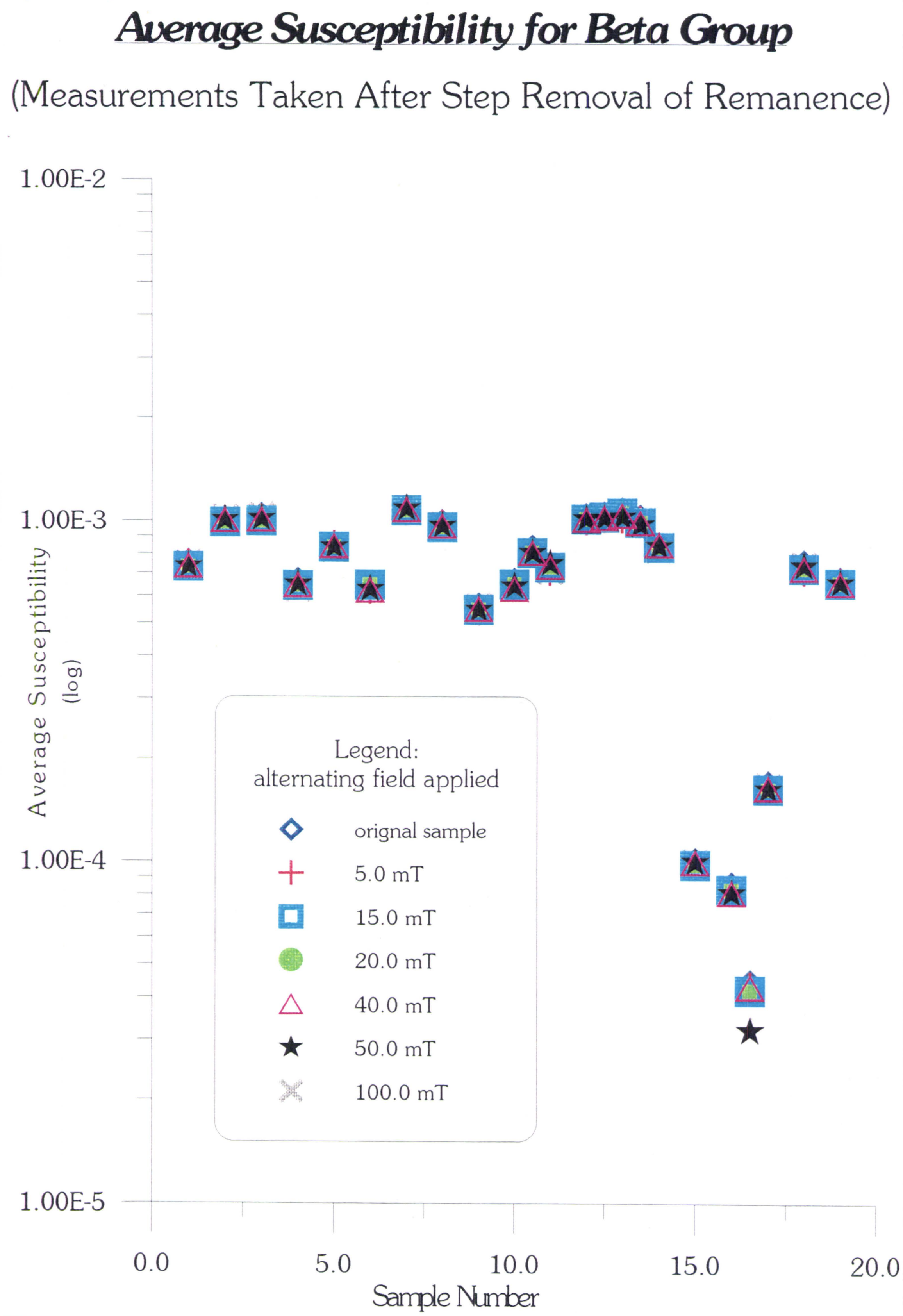

Figure Twenty-Five:

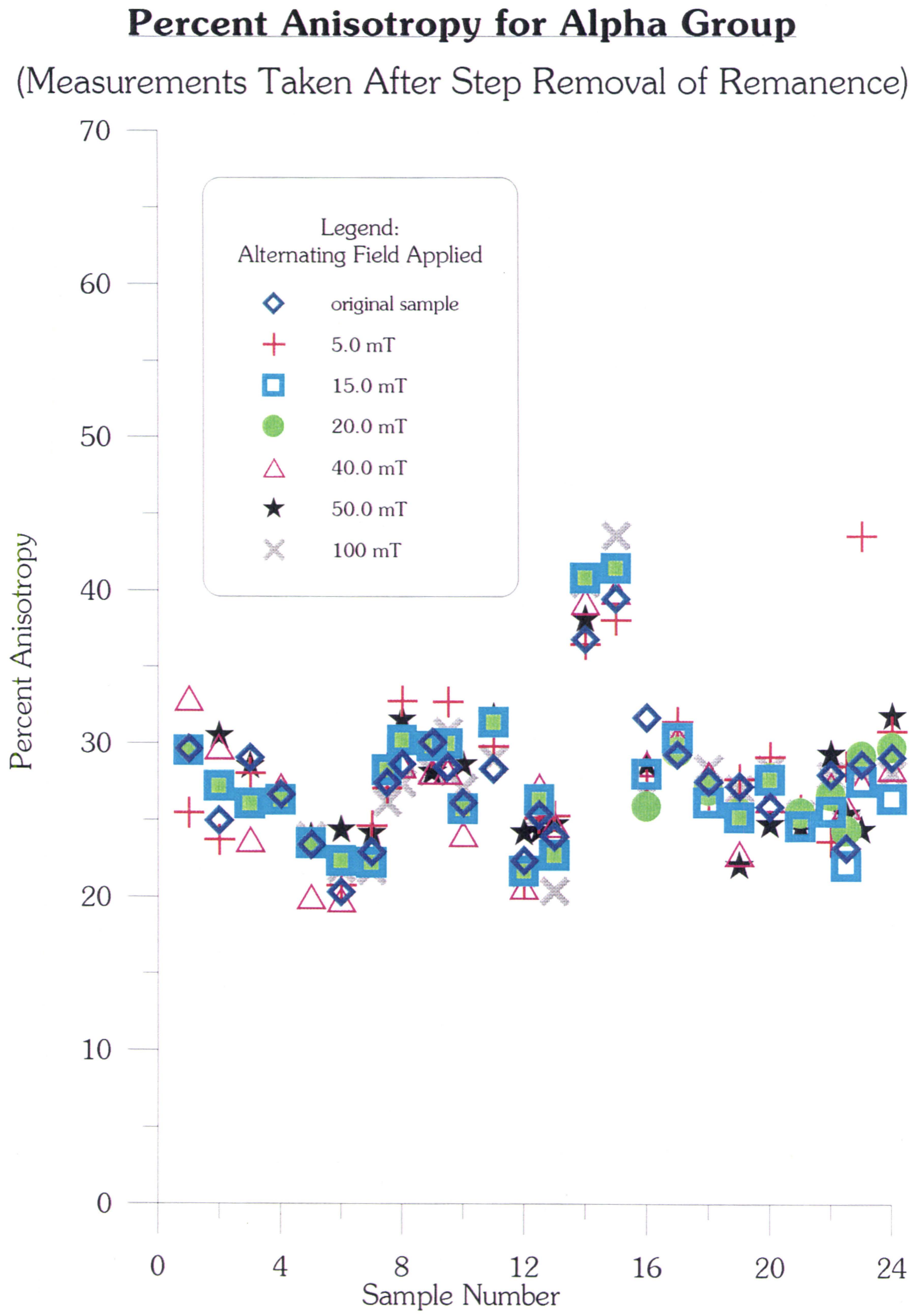

Figure Twenty-Six:

Percent Anisotropy for Beta Group

(Measurements Taken After Step Removal of Remanence)

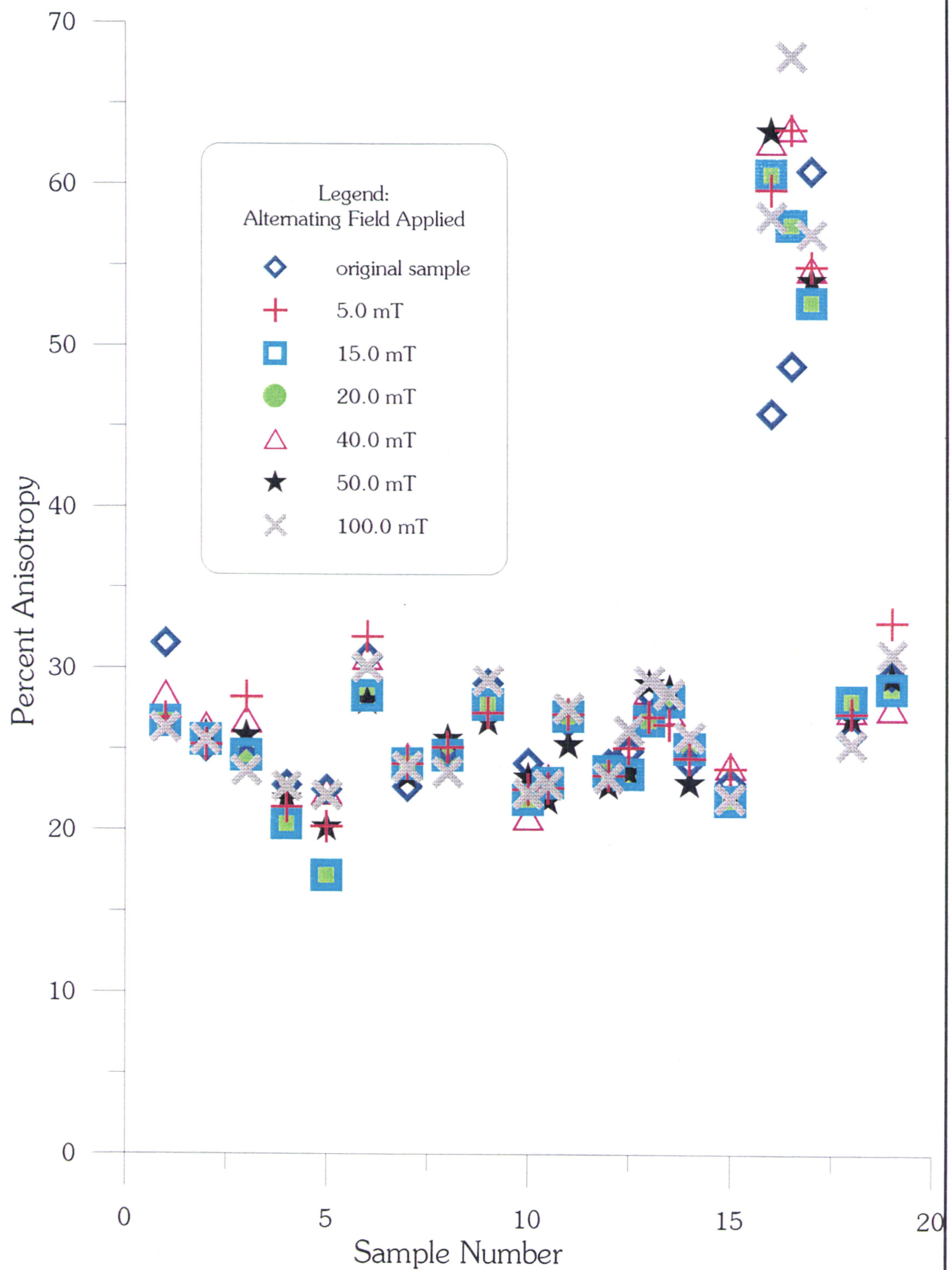

Figure Twenty-Seven: Alpha, number 6

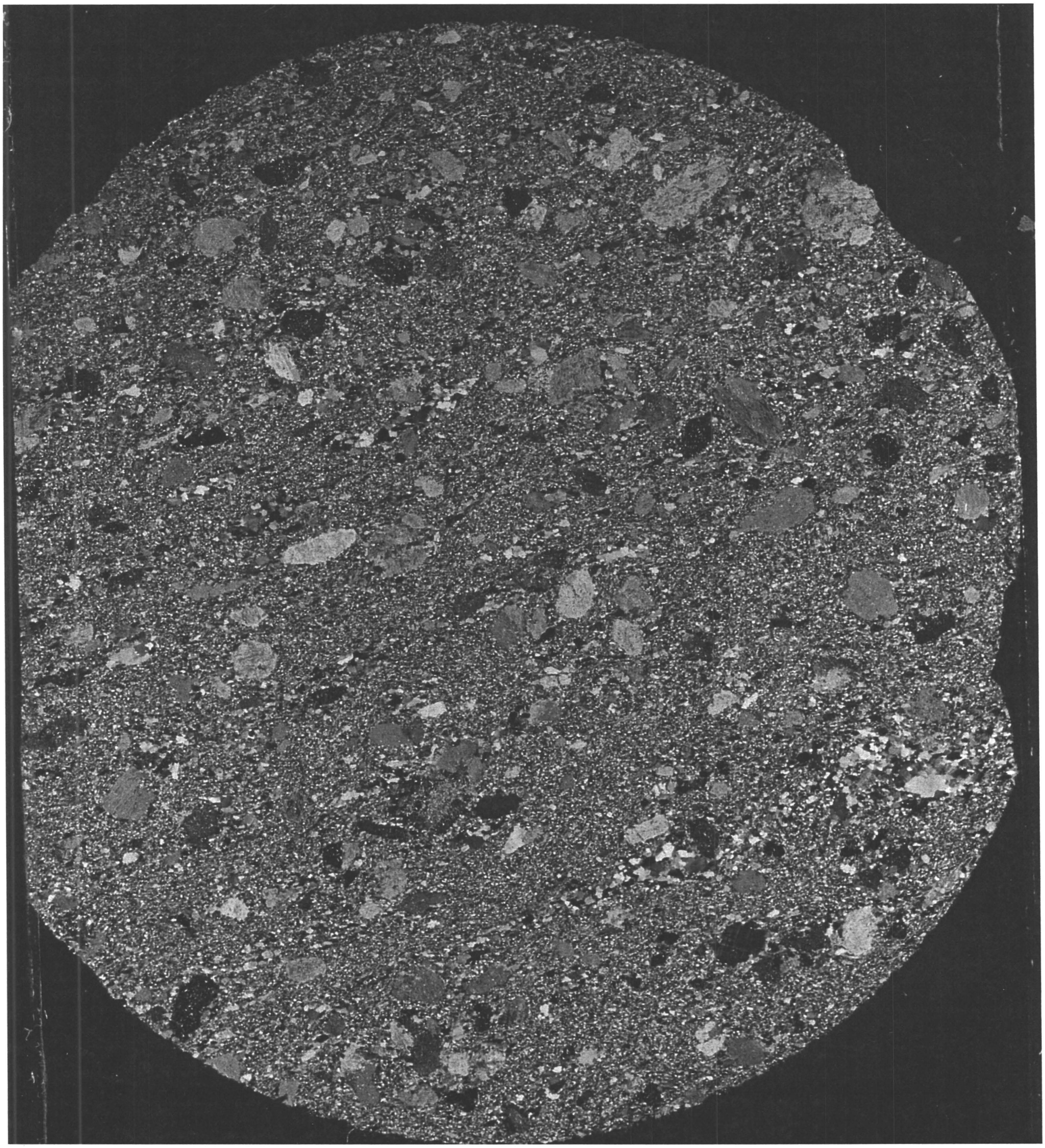

Figure Twenty-Eight: Alpha, number 12

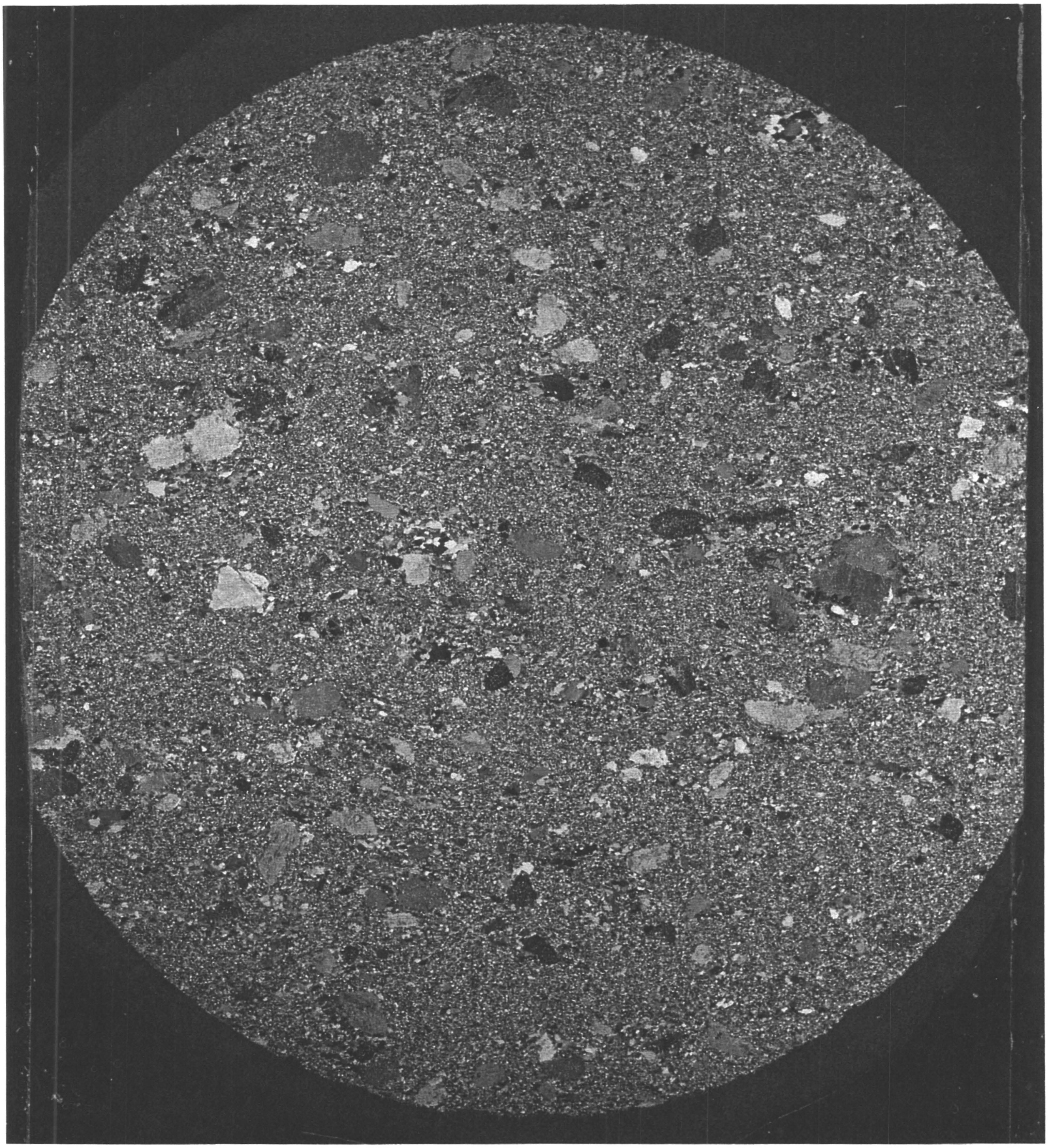

Figure Twenty-Nine: Alpha, number 15
(Recrystallization indicated by arrow, notice matrix surrounding the mineral recrystallization)

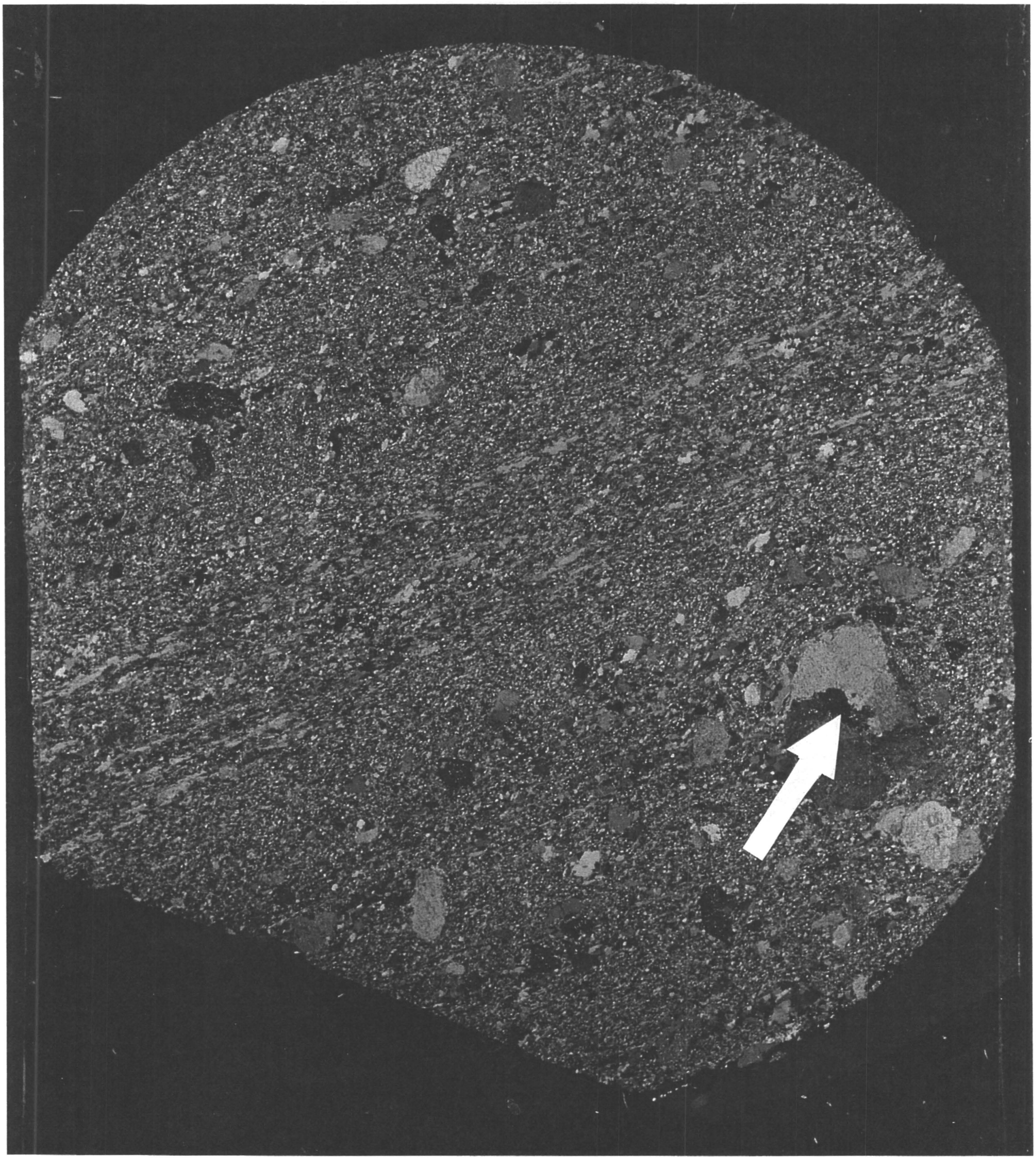

Figure Thirty: Beta, number 13

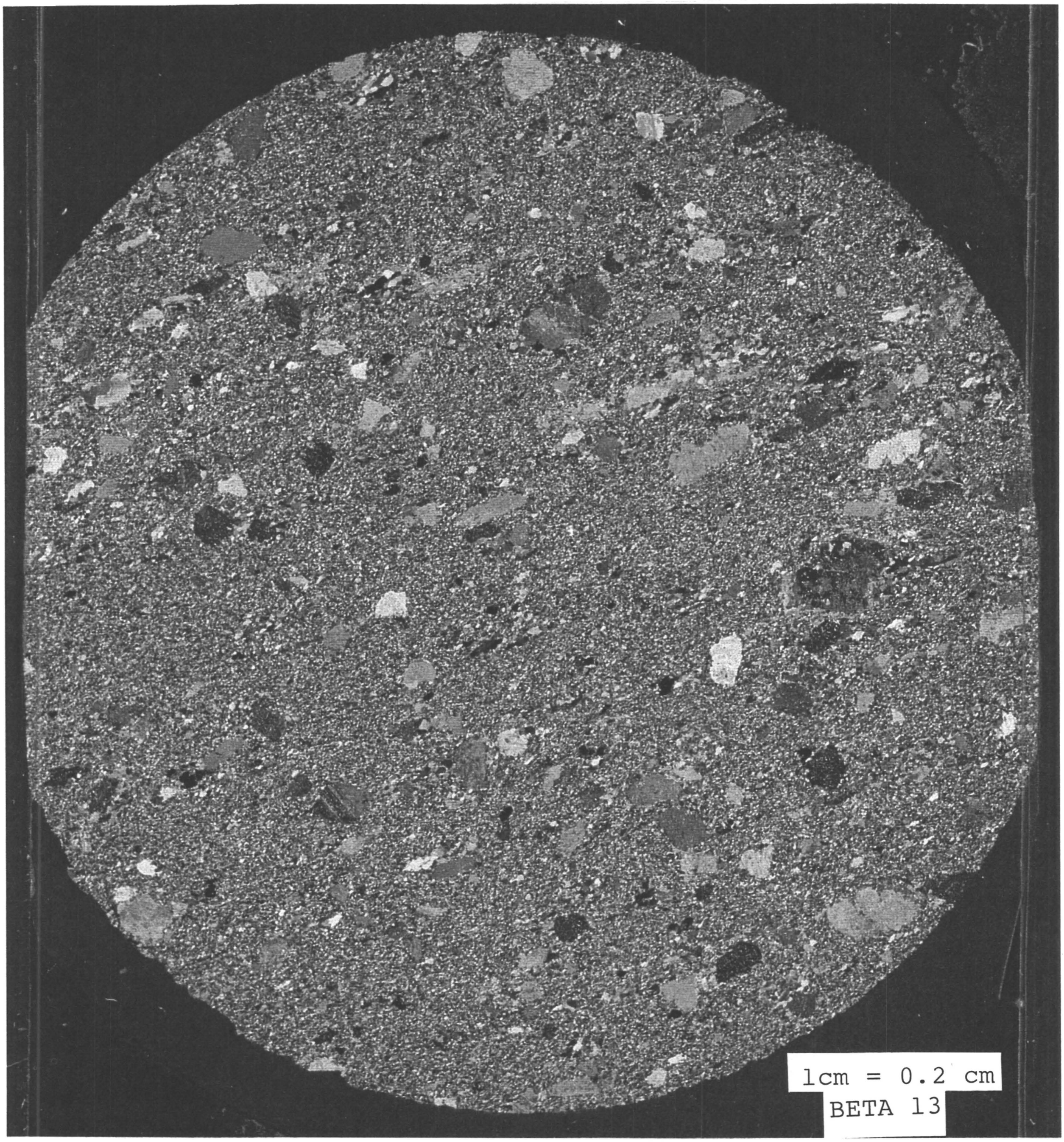

Figure Thirty-One: Beta, number 12

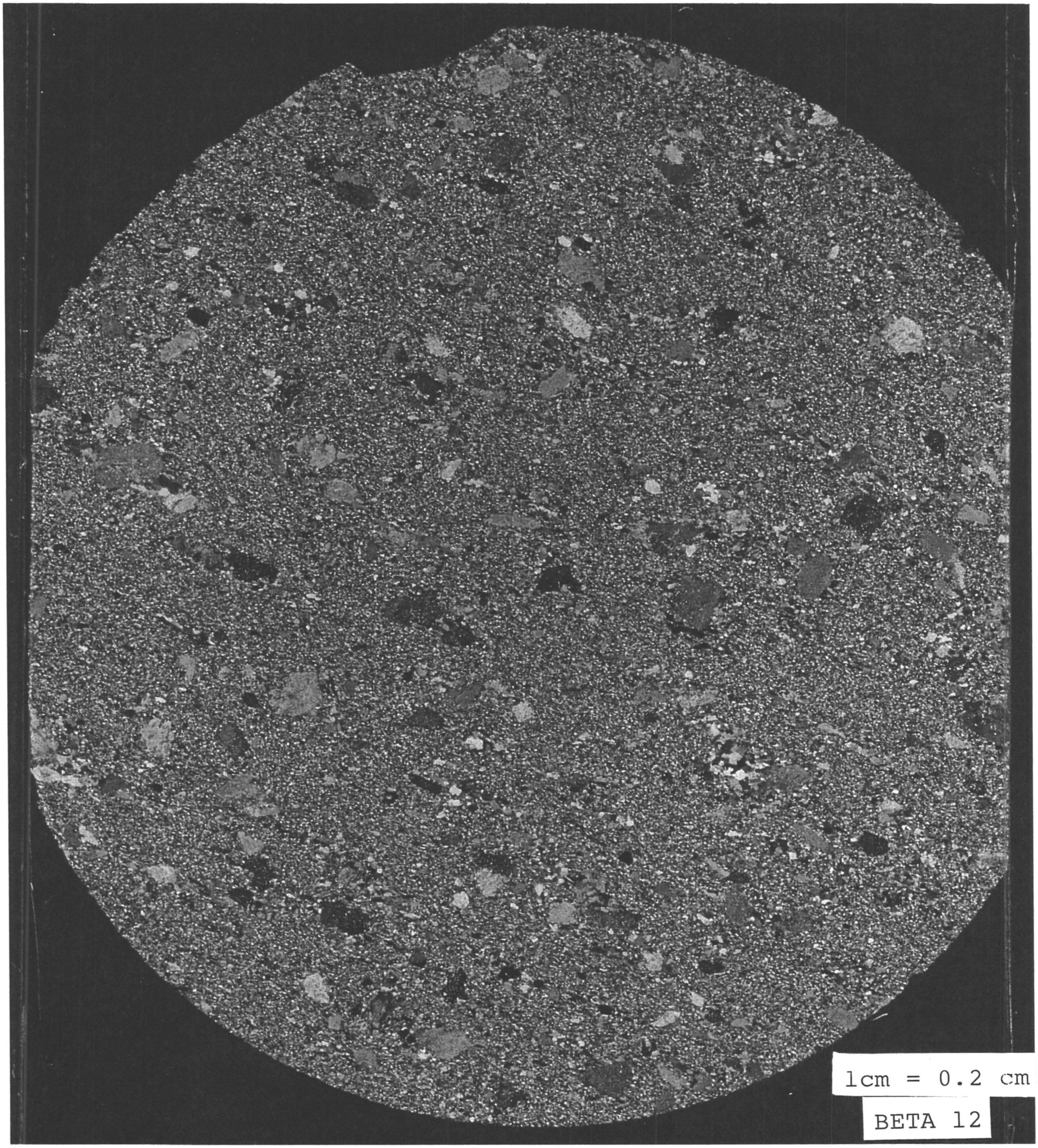

Figure Thirty-Two: Beta, number 16

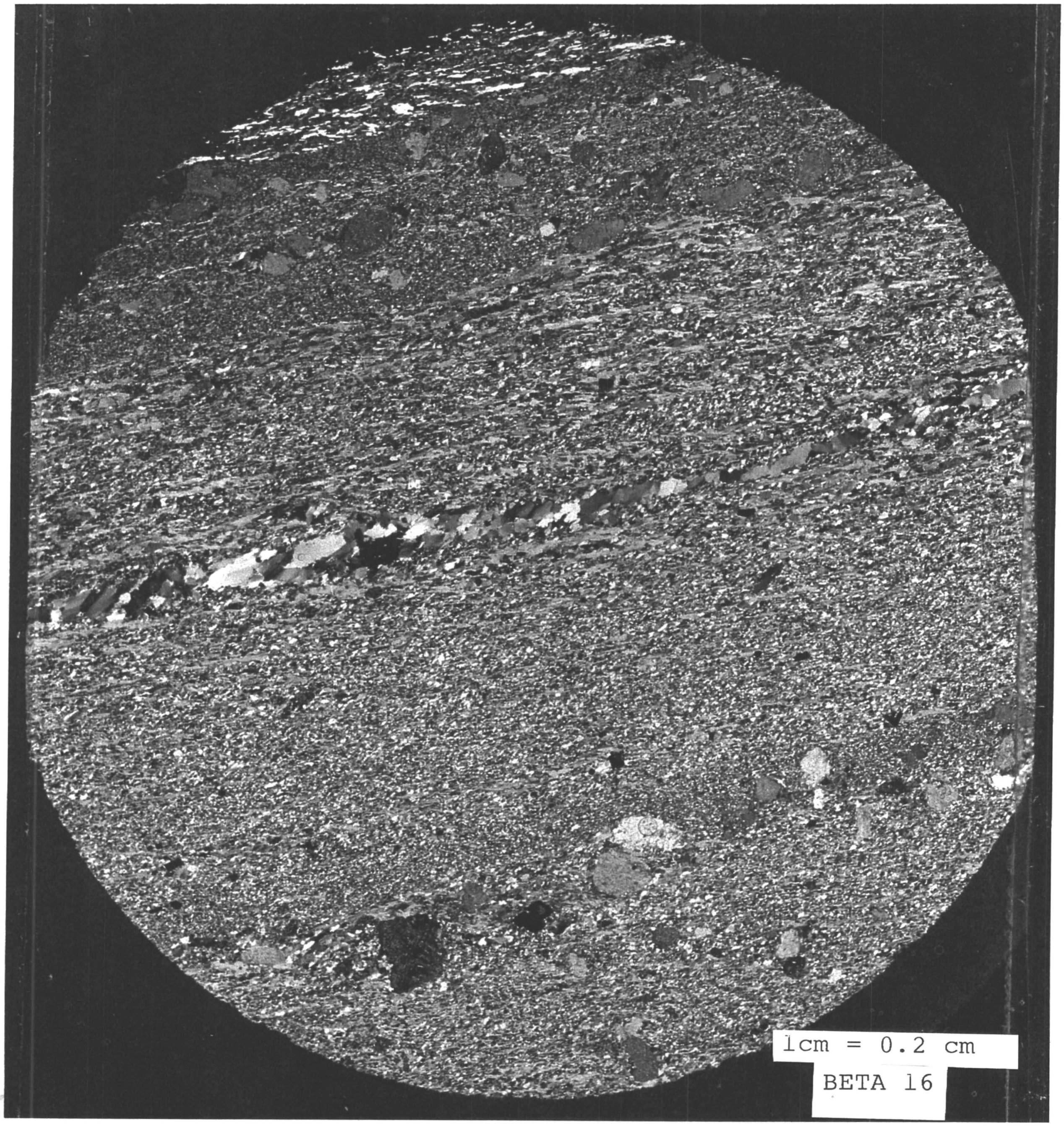

Figure Thirty-Three: Beta, number 19

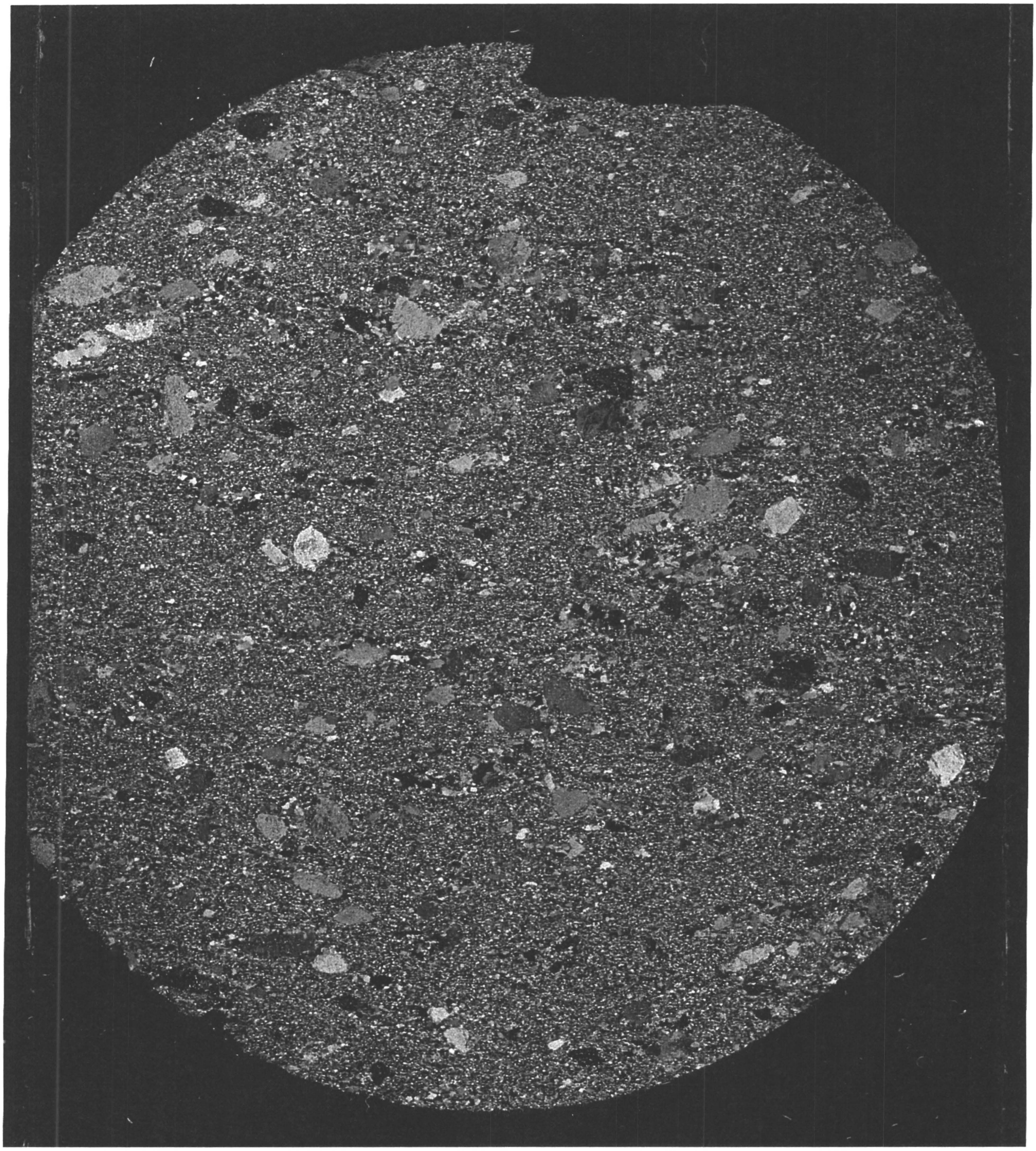

grains which are more rounded and elongated (figure 27, Alpha - sample 6), where others show complete randomness even though the matrix has a preferred orientation (figure 28, Alpha - sample 12).

It is evident that all the samples have undergone a regional deformation, which is seen from the matrix of reduced grain size. Larger anhedral to subhedral grains are also prominent in many of the samples. Further deformation is indicated by further reduction of the grain size in the matrix, absence of larger grains and recrystallization (figure 29, Alpha - sample 15).

Utilizing a microscope at 40X magnification, the general mineralogy is seen to be typical of a granite, with biotite, muscovite, K-feldspar, plagioclase, quartz, hornblende. The opaque minerals present were magnetite, hematite and kaersutite. K-feldspars were the most abundant large minerals, where biotite was the second most abundant. Chlorite is also seen in many thin sections, a common hydrothermal alteration of biotite and amphiboles.

Magnetite occurs as small (0.05 to 0.3 mm) anhedral to subhedral grains. Their occurrence in the samples is significant, in that their magnetic interaction is expected to contribute to the magnetic fabric. Kaersutite (magnetite with high titanium content), is also considered a contributor to the magnetic fabric. It is present in every thin section and identified by its reddish brown colour in contrast to the opaques.

The data which was collected from the Image Analyzer provided results similar to what could be seen in the photographs and were not used. Parameters that were measured using the Northern Exposure program were: object area, object perimeter, minimum (x,y), length (x,y), shortest chord and orientation. It should be noted again that these measurements are for only the two dimensional view of the thin section; thus the true maximum and minimum measurement may be different.

DISCUSSION:

Relationship of Magnetic Fabric and Deformation:

From AMS the bulk susceptibility and percent anisotropy were measured. There is no significant change across the study areas other than sample 14, 15 and 17 in Alpha and sample 16a, 16b and 17 in Beta. It is important to determine what kind of environment would cause a low bulk susceptibility but a high anisotropy. To reduce the susceptibility of the rock sample, the grain size would have to be reduced in order to diminish the intensity of the magnetic minerals contribution. This grain size reduction may occur during brittle deformation where the grains are rotated against one another and thus broken down to create a uniform subrounded matrix. If this area continues to undergo a deformation which becomes more ductile then the alignment of the grains becomes more uniform and any recrystallization occurring will take place to yield a significant preferred orientation. This greater alignment of the crystals would therefore increase the anisotropy. In both Alpha and Beta areas the low bulk susceptibilities are matched by high percent anisotropy, suggesting that this kind of deformation has occurred. Sample 16 in the Beta group displays the lowest bulk susceptibility and one of the highest percent anisotropy indicating an area where very intense localized deformation has occurred. If a closer look is taken at the graphs, it is noted that the low bulk susceptibilities also match with low anisotropies, except in the extreme cases. Thus a correlation can be established that low strain deformation can alter the magnetic fabric and be recorded on a fine scale, but the more intense deformational processes leave a stronger and more distinct magnetic signature.

An important aspect to notice from these graphs relative to the samples collected, is that there are other regions in the study areas which have a high concentration of mylonite bands and fracturing. This could only lead to the conclusion that two types of mylonitization have taken place. One type which would be able to overprint the regional fabric and a second type in which mylonitization has progressed so as to increase the percent anisotropy and reduce the susceptibility. This second type may be responsible for reduction of grain size, increased alignment and new magnetite development. From this study it is apparent that this type of mylonitization is only developed in a localized region in the Beta group, seen in sample 16.

Now that it is shown that deformation can combine or overprint the regional fabric, it is necessary to take a closer look at the magnetic foliation and lineation. These characteristics are seen from the stereonets where the k1, k2 and k3 axes where plotted. Regional foliation is determined to be in the general southwest northeast direction. The dips of the foliations go through the vertical axis, but this may be due to the process of uplifting the mylonites from depth. The stereonets which represent the more deformed regions have much more intense foliations and lineations and have a tighter cluster of data points. By plotting the axis, regions of high deformation can be seen by the change in orientation of the foliation and an increased dip direction. Thus it is possible to see indications of deformation by measuring the magnetic fabric of the minerals present in the rock samples.

Remanence:

Remanence was measured to determine if AMS measurements were from Natural Remanent Magnetization (NRM) or a secondary processes, giving rise to Chemical Remanent Magnetization, Thermal Remanent Magnetization, etc. From the results measured, susceptibility, percent anisotropy and k1, k2 and k3 axes, it is clear that NRM is the responsible magnetization.

Figures 20 and 21, of Alpha and Beta remanence measurements, indicate a equal orientation of North and South trends in the down line perspective. This is also seen in the plotting of the stereonets by the dip changing through the vertical axis when utilizing the right hand rule, as all this data does. Variance is seen in the West - East view, from the profile perspective, and is significant where the fractures and mylonites occur, thus indicating a physical change of the NRM orientation

ARM/X versus the sample number demonstrates where finer grains may be generated in the samples. It is due to the relationship of ARM (anhysteretic Remanent magnetization) and susceptibility, which are related to grain size. Finer grain size in figure twenty-one is shown by the higher values. Reduction of grain size is likely to develop in brittle deformation and would thus be expected to be to found in areas of fracturing. Its occurrence is not always expected to be present in mylonitization zones, as this process often signifies flow, a more ductile then brittle deformational process.

Relationship of Petrological Fabric and Deformation:

Deformation is evident in the thin sections from the reduced grain size, greater alignment of the grains and absence of larger minerals (which are present in the less deformed sections). Inspecting the thin sections which represent the regional mineralogy was determined to consist of biotite, muscovite, k-feldspar, quartz, plagioclase, and opaque minerals such as magnetite and kaersutite. The larger grains which are seen in the fine grained matrix are dominantly k-feldspar, in which some have muscovite inclusions, indicating recrystallization. Recrystallization is also indicated by the matrix which surrounds the mineral recrystallizing being pushed out in a radial pattern, shown in figure 29.

The thin sections which represent a higher state of deformation show a greater alignment, compare figure 30 (low deformation) and figure 31 (intermediate deformation). The majority of the matrix and the larger minerals are elongate and in a preferred orientation. In some areas the grain size is further reduced , but overall it does not show a different fabric from the regional other then an increased mineral alignment. As the samples get closer to regions of higher intensities of deformation in the study areas, more variances are seen in the fabric, figure 32. Further reduction of the grain size is apparent and there are no longer any larger minerals present. The alignment of minerals is accentuated any recrystallization has occurred in a preferred orientation. In figure 31 recrystallization is seen in the middle which has undergone subsequent shear, recognized by the Riedel shear indicating a sinistral shear from this thin section's perspective. High degrees of deformation are seen in other thin sections, by the absence of larger mineral grains, greatly reduced grain size and increased alignment, but only this thin section displayed such an advanced stage of recrystallization.

Correlation with Magnetic and Petrological Fabric:

In this study, a relationship has been established that magnetic fabric changes as the deformation intensities change, as shown by the petrological fabric. It is important to further extend this association, to see if magnetic fabric and petrological fabric relate to each other. As the deformation intensity increases, changes are seen in both the petrological and magnetic fabric, but are these changes similar? First sample 16 in the Beta group, figure 32, is analyzed to ascertain a correlation between the two. Both the petrological and magnetic fabrics demonstrate intense deformation and have very similar preferred orientations in their fabric. Figure 34 shows the magnetic foliation and lineations of this sample and its location on the study area map. In this case, a correlation is apparent, yet in some examples (Beta, sample 19, figure 33) this is not the case. An explanation for this may be due to the recrystallization of magnetite grains increasing their percent volume and their increased size changing the magnetic orientation. Overall the preferred orientation of the magnetic and

Figure Thirty-Four:

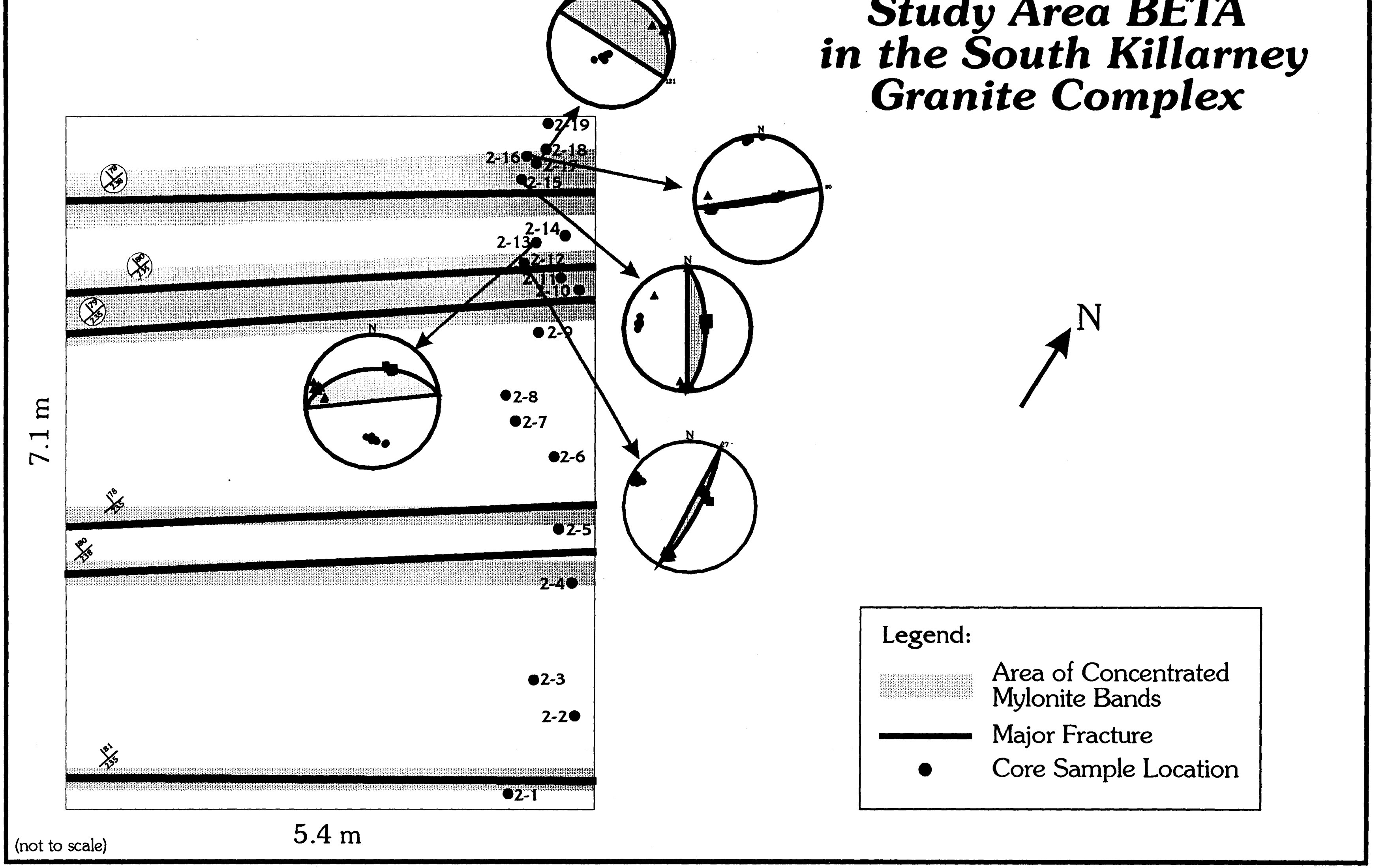

petrological fabric are similar, suggesting that by utilizing both fabrics, regions of high deformation can be seen on a microscopical scale.

CONCLUSIONS:

Strain deformation can be seen in both magnetic and petrological fabric. The fabric orientation becomes more intense as the deformation intensity increases. This intensity is seen in the magnetic fabric foliation and lineation and in the petrology by the increased alignment. Both fabrics are therefore good indicators of deformation and to the extent has it occurred. Previous studies have also correlated this data on a regional scale where this study has shown the relationship on a much finer scale. The importance of establishing this relationship on any scale, is to aid in the identification of a deformational event and its extent in the field when it is not otherwise easily recognisable.

Future Work:

This study only encompassed two small areas approximately six metres by six metres. It would be advisable, to further this study, by taking additional samples closer to and on the Grenville Front to determine any change in the regional magnetic fabric. This may aid in determining the timing of the mylonite uplift relative to the Grenville Front. Samples should also be collected in the northern region of the Killarney Igneous Complex to see if the regional magnetic and petrological fabrics are similar. If there is a similarity, then this would indicate a large regional tectonic deformation. If no similarity is found then the deformation has been localised in the southern region of the complex and an explanation would have to be determined which would cause only partial deformation in this plutonic body.

REFERENCES:

Benn, Keith. 1994. Overprinting of magnetic fabrics in granites by small strains: numerical modelling. *Tectonophysics,* 233: 153-162.

Birch, Francis S. 1979. Magnetic fabric of the Exeter Pluton, New Hampshire. *Journal of Geophysical Research*, 84: 1129-1137.

Cruden, Alexander R. and Launeau Patrick. 1994. Structure, magnetic fabric and emplacement of the Archean Lebel Stock, SW Abitibi Greenstone Belt. *Journal of Structural Geology*, 16: 677-691.

Davis, P.M. and Evans, M.E. 1976. Interacting single-domain properties of magnetite intergrowths. *Journal of Geophysical Research*, 81: 989-994.

Fan, Ximo. 1995. Structural Studies of the Killarney Igneous Complex, Ontario and their Tectonic Implications. PhD thesis, McMaster University, Hamilton, Ontario. 208 pgs.

Hargraves, R.B., Johnson, D. and Chan, C.Y. 1991. Distribution anisotropy: the cause of AMS in igneous rocks? *Geophysical Research Letters*, 18: 2193-2196.

Hirt, A.M., Lowrie, W., Clendenen, W.S. and Kligfield R. 1993. Correlation of strain and the anisotropy of magnetic susceptibility in the Onaping Formation: evidence for a near-circular origin of the Sudbury Basin. *Tectonophysics*, 225: 231-254.

King, J., Banerjee, S.K., Marvin, J. and Ozdemir, O. 1982. A comparison of different magnetic methods for determining the relative grain size of magnetite in natural materials: some results from lake sediments. *Earth and Planetary Science Letters*, 59: 404-419.

Park, John K., Tanczyk, Elizabeth L. and Desbarats, Alexandre. 1988. Magnetic fabric and its significance in the 1400 Ma Mealy Diabase Dykes of Labrador, Canada. *Journal of Geophysical Research*, 93: 13,689-13,704.

Van Breemen, O. And Davidson, A. 1988. Northeast extension of Proterozoic terranes of midcontinental North America. *Geological Society of the American Bulletin*, 100: 630-638.

Wanless, R.K., and Loveridge, W.D. 1972. Rubidium-Strontium isochron age studies. Report 1: Geological Survey of Canada, paper 72-23, 77pgs.

Wiacek, Andrew. A paleomagnetic analysis of the deformation and hydrothermal alteration in the Killarney igneous complex, Ontario. MSc thesis, McMaster University, Hamilton, Ontario. 195 pgs.

APPENDIX

Sample - Alpha demagnetised in alternating field of 5.0 mT
Indicates ARM-BAR conversion to bulk susceptibility, percent anisotropy, maximum, intermediate and minimum axis and values for P1, P2 and P3.

Specimen Number : 1-1 Core Decl = 345.0 Core Incl = 77.0

Axis	Dec	Inc	Magnitude
Min:	238.1	80.0	0.000865
Int:	66.6	9.9	0.001057
Max:	336.4	1.5	0.001123

Av Susc = 0.001015 % Anisotropy = 25.46
Lin = 0.065 Fol = 0.222 Q = 0.291 E = 1.152
P1 = 1.06204 P2 = 1.29887 P3 = 1.22299

Specimen Number : 1-2 Core Decl = 334.0 Core Incl = 72.0

Axis	Dec	Inc	Magnitude
Min:	170.3	69.9	0.000881
Int:	44.9	12.0	0.001026
Max:	311.4	15.9	0.001121

Av Susc = 0.001009 % Anisotropy = 23.72
Lin = 0.094 Fol = 0.190 Q = 0.494 E = 1.066
P1 = 1.09239 P2 = 1.27168 P3 = 1.16413

Specimen Number : 1-3 Core Decl = 31.0 Core Incl = 78.0

Axis	Dec	Inc	Magnitude
Min:	214.4	20.1	0.000773
Int:	120.4	10.8	0.000935
Max:	3.8	67.0	0.001029

Av Susc = 0.000912 % Anisotropy = 28.06
Lin = 0.103 Fol = 0.229 Q = 0.450 E = 1.099
P1 = 1.10053 P2 = 1.33125 P3 = 1.20965

Specimen Number : 1-4 Core Decl = 124.0 Core Incl = 77.0

Axis	Dec	Inc	Magnitude
Min:	47.9	61.0	0.000664
Int:	193.4	24.5	0.000781
Max:	290.2	14.4	0.000870

Av Susc = 0.000772 % Anisotropy = 26.65
Lin = 0.115 Fol = 0.209 Q = 0.552 E = 1.055
P1 = 1.11392 P2 = 1.30965 P3 = 1.17571

Specimen Number : 1-5 Core Decl = 111.0 Core Incl = 86.0

Axis	Dec	Inc	Magnitude
Min:	46.4	83.4	-0.000003
Int:	179.1	4.5	0.000748
Max:	269.5	4.8	0.000813

Av Susc = 0.000519 % Anisotropy = 157.10
Lin = 0.125 Fol = 1.508 Q = 0.083 E = -235.278
P1 = 1.08681 P2 = -277.89914 P3 = -255.70208

Specimen Number : 1-6 Core Decl = 161.0 Core Incl = 84.0

Axis	Dec	Inc	Magnitude
Min:	16.2	76.4	0.000551
Int:	106.8	0.1	0.000650
Max:	196.8	13.6	0.000682

Av Susc = 0.000628 % Anisotropy = 20.77
Lin = 0.050 Fol = 0.183 Q = 0.275 E = 1.125
P1 = 1.04839 P2 = 1.23643 P3 = 1.17936

Specimen Number : 1-7a Core Decl = 155.0 Core Incl = 85.0

Axis	Dec	Inc	Magnitude
Min:	8.8	66.4	0.000724
Int:	247.3	12.9	0.000883
Max:	152.6	19.4	0.000932

Av Susc = 0.000846 % Anisotropy = 24.65
Lin = 0.058 Fol = 0.218 Q = 0.266 E = 1.156
P1 = 1.05545 P2 = 1.28830 P3 = 1.22062

Specimen Number : 1-7b Core Decl = 155.0 Core Incl = 85.0

Axis	Dec	Inc	Magnitude
Min:	18.5	73.8	0.000742
Int:	231.2	13.7	0.000951
Max:	139.1	8.4	0.000984

Av Susc = 0.000892 % Anisotropy = 27.08
Lin = 0.036 Fol = 0.253 Q = 0.144 E = 1.240
P1 = 1.03406 P2 = 1.32562 P3 = 1.28195

Specimen Number : 1-8 Core Decl = 112.0 Core Incl = 83.0

Axis	Dec	Inc	Magnitude
Min:	80.4	63.1	0.000583
Int:	173.4	1.5	0.000717
Max:	264.2	26.9	0.000813

Av Susc = 0.000704 % Anisotropy = 32.74
Lin = 0.137 Fol = 0.259 Q = 0.527 E = 1.085
P1 = 1.13420 P2 = 1.39573 P3 = 1.23059

Specimen Number : 1-9a Core Decl = 21.0 Core Incl = 84.0

Axis	Dec	Inc	Magnitude
Min:	189.9	38.1	0.000918
Int:	94.5	6.9	0.001087
Max:	355.9	51.1	0.001235

Av Susc = 0.001080 % Anisotropy = 29.36
Lin = 0.137 Fol = 0.225 Q = 0.611 E = 1.042
P1 = 1.13652 P2 = 1.34535 P3 = 1.18374

Specimen Number : 1-9b   Core Decl = 21.0   Core Incl = 84.0

Axis	Dec	Inc	Magnitude
Min:	204.4	30.3	0.000851
Int:	302.4	13.4	0.001052
Max:	53.4	56.3	0.001187

Av Susc = 0.001030   % Anisotropy = 32.69
Lin = 0.131   Fol = 0.261   Q = 0.502   E = 1.096
P1 = 1.12835   P2 = 1.39590   P3 = 1.23712

Specimen Number : 1-10   Core Decl = 25.0   Core Incl = 86.0

Axis	Dec	Inc	Magnitude
Min:	202.4	16.1	0.000702
Int:	298.5	20.2	0.000864
Max:	76.6	63.7	0.000914

Av Susc = 0.000827   % Anisotropy = 25.62
Lin = 0.060   Fol = 0.226   Q = 0.268   E = 1.163
P1 = 1.05789   P2 = 1.30163   P3 = 1.23041

Specimen Number : 1-11   Core Decl = 97.0   Core Incl = 84.0

Axis	Dec	Inc	Magnitude
Min:	94.4	60.0	0.000817
Int:	348.3	9.1	0.000961
Max:	253.4	28.3	0.001104

Av Susc = 0.000961   % Anisotropy = 29.80
Lin = 0.149   Fol = 0.224   Q = 0.666   E = 1.023
P1 = 1.14881   P2 = 1.35014   P3 = 1.17526

Specimen Number : 1-12a   Core Decl = 135.0   Core Incl = 78.0

Axis	Dec	Inc	Magnitude
Min:	17.5	71.3	0.000625
Int:	246.5	12.5	0.000752
Max:	153.4	13.7	0.000774

Av Susc = 0.000717   % Anisotropy = 20.83
Lin = 0.031   Fol = 0.193   Q = 0.158   E = 1.170
P1 = 1.02910   P2 = 1.23903   P3 = 1.20399

Specimen Number : 1-12b   Core Decl = 135.0   Core Incl = 78.0

Axis	Dec	Inc	Magnitude
Min:	15.5	79.2	0.000771
Int:	204.9	10.6	0.000934
Max:	114.6	1.7	0.000997

Av Susc = 0.000901   % Anisotropy = 25.14
Lin = 0.070   Fol = 0.217   Q = 0.322   E = 1.136
P1 = 1.06719   P2 = 1.29385   P3 = 1.21240

Specimen Number : 1-13 Core Decl = 327.0 Core Incl = 84.0

Axis	Dec	Inc	Magnitude
Min:	153.2	78.3	0.000762
Int:	58.6	0.9	0.000899
Max:	328.4	11.6	0.000985

Av Susc = 0.000882 % Anisotropy = 25.27
Lin = 0.098 Fol = 0.204 Q = 0.481 E = 1.076
P1 = 1.09608 P2 = 1.29236 P3 = 1.17908

Specimen Number : 1-14 Core Decl = 193.0 Core Incl = 69.0

Axis	Dec	Inc	Magnitude
Min:	58.7	34.1	0.000218
Int:	321.8	10.1	0.000292
Max:	217.6	54.0	0.000319

Av Susc = 0.000276 % Anisotropy = 36.47
Lin = 0.098 Fol = 0.316 Q = 0.311 E = 1.224
P1 = 1.09281 P2 = 1.46189 P3 = 1.33774

Specimen Number : 1-15 Core Decl = 179.0 Core Incl = 70.0

Axis	Dec	Inc	Magnitude
Min:	41.2	35.1	0.000203
Int:	304.1	10.1	0.000275
Max:	200.4	53.1	0.000302

Av Susc = 0.000260 % Anisotropy = 38.07
Lin = 0.102 Fol = 0.330 Q = 0.308 E = 1.239
P1 = 1.09598 P2 = 1.48798 P3 = 1.35767

Specimen Number : 1-16 Core Decl = 306.0 Core Incl = 81.0

Axis	Dec	Inc	Magnitude
Min:	343.1	86.4	0.000812
Int:	236.0	1.1	0.000949
Max:	145.9	3.5	0.001070

Av Susc = 0.000944 % Anisotropy = 27.31
Lin = 0.128 Fol = 0.209 Q = 0.609 E = 1.038
P1 = 1.12675 P2 = 1.31739 P3 = 1.16920

Specimen Number : 1-17 Core Decl = 209.0 Core Incl = 73.0

Axis	Dec	Inc	Magnitude
Min:	17.5	5.1	0.000363
Int:	110.8	32.7	0.000432
Max:	279.7	56.8	0.000498

Av Susc = 0.000431 % Anisotropy = 31.42
Lin = 0.152 Fol = 0.238 Q = 0.638 E = 1.036
P1 = 1.15141 P2 = 1.37353 P3 = 1.19292

Specimen Number : 1-18   Core Decl = 354.0   Core Incl = 84.0

Axis	Dec	Inc	Magnitude
Min:	178.4	45.9	0.000807
Int:	70.0	17.0	0.000947
Max:	325.6	39.2	0.001056

Av Susc = 0.000937   % Anisotropy = 26.58
Lin = 0.116   Fol = 0.208   Q = 0.557   E = 1.053
P1 = 1.11456   P2 = 1.30853   P3 = 1.17404

Specimen Number : 1-19   Core Decl = 111.0   Core Incl = 78.0

Axis	Dec	Inc	Magnitude
Min:	103.4	65.8	0.000681
Int:	359.1	6.3	0.000804
Max:	266.4	23.2	0.000902

Av Susc = 0.000796   % Anisotropy = 27.69
Lin = 0.123   Fol = 0.216   Q = 0.569   E = 1.052
P1 = 1.12148   P2 = 1.32338   P3 = 1.18004

Specimen Number : 1-20   Core Decl = 229.0   Core Incl = 79.0

Axis	Dec	Inc	Magnitude
Min:	211.7	6.2	0.000588
Int:	119.9	15.3	0.000756
Max:	323.0	73.4	0.000796

Av Susc = 0.000713   % Anisotropy = 29.13
Lin = 0.057   Fol = 0.263   Q = 0.217   E = 1.219
P1 = 1.05376   P2 = 1.35314   P3 = 1.28411

Specimen Number : 1-21   Core Decl = 311.0   Core Incl = 81.0

Axis	Dec	Inc	Magnitude
Min:	75.9	81.3	0.000091
Int:	271.4	8.3	0.000100
Max:	181.1	2.3	0.000117

Av Susc = 0.000103   % Anisotropy = 25.73
Lin = 0.168   Fol = 0.174   Q = 0.966   E = 0.940
P1 = 1.17207   P2 = 1.29101   P3 = 1.10147

Specimen Number : 1-22a   Core Decl = 17.0   Core Incl = 82.0

Axis	Dec	Inc	Magnitude
Min:	205.5	43.5	0.000853
Int:	95.8	19.6	0.000979
Max:	348.4	40.0	0.001083

Av Susc = 0.000972   % Anisotropy = 23.65
Lin = 0.107   Fol = 0.183   Q = 0.581   E = 1.038
P1 = 1.10567   P2 = 1.26945   P3 = 1.14812

Specimen Number : 1-22b   Core Decl = 17.0   Core Incl = 82.0

Axis	Dec	Inc	Magnitude
Min:	160.8	75.1	0.000883
Int:	280.0	7.4	0.001121
Max:	11.7	12.9	0.001186

Av Susc = 0.001063   % Anisotropy = 28.52
Lin = 0.061   Fol = 0.255   Q = 0.239   E = 1.201
P1 = 1.05783   P2 = 1.34349   P3 = 1.27004

Specimen Number : 1-23   Core Decl = 337.0   Core Incl = 81.0

Axis	Dec	Inc	Magnitude
Min:	160.7	44.4	0.000785
Int:	18.1	39.0	0.001132
Max:	271.2	19.7	0.001244

Av Susc = 0.001053   % Anisotropy = 43.56
Lin = 0.106   Fol = 0.383   Q = 0.277   E = 1.313
P1 = 1.09868   P2 = 1.58474   P3 = 1.44240

Specimen Number : 1-24   Core Decl = 41.0   Core Incl = 85.0

Axis	Dec	Inc	Magnitude
Min:	231.6	18.9	0.000741
Int:	132.1	25.7	0.000919
Max:	353.8	57.2	0.001016

Av Susc = 0.000892   % Anisotropy = 30.81
Lin = 0.109   Fol = 0.254   Q = 0.428   E = 1.122
P1 = 1.10541   P2 = 1.37083   P3 = 1.24011